Earth-Science Reviews 107 (2011) 107–122

Contents lists available at ScienceDirect

Earth-Science Reviews

journal homepage: www.elsevier.com/locate/earscirev

Expanding the proxy toolkit to help identify past events — Lessons from the 2004 Indian Ocean Tsunami and the 2009 South Pacific Tsunami

Catherine Chagué-Goff [a,b,*], Jean-Luc Schneider [c], James R. Goff [a], Dale Dominey-Howes [a], Luke Strotz [a]

[a] Australian Tsunami Research Centre and Natural Hazards Research Laboratory, School of Biological, Environmental and Earth Sciences, University of New South Wales, Sydney NSW 2052, Australia
[b] Institute for Environmental Research, Australian Nuclear Science and Technology Organisation, Locked Bag 2001, Kirrawee DC, NSW 2232, Australia
[c] Université Bordeaux 1, CNRS-UMR 5805 «EPOC», Bâtiment B18, Avenue des Facultés, F-33405 Talence Cedex, France

ARTICLE INFO

Article history:
Received 31 July 2010
Accepted 18 March 2011
Available online 24 March 2011

Keywords:
2009 South Pacific Tsunami
proxies
toolkit
chemical proxies
anisotropy of magnetic susceptibility
heavy minerals

ABSTRACT

Some of the proxies used to identify palaeotsunamis are reviewed in light of new findings following the 2004 Indian Ocean Tsunami and the 2009 South Pacific Tsunami, and a revised toolkit provided. The new application of anisotropy of magnetic susceptibility (AMS) to the study of tsunami deposits and its usefulness to determine the hydrodynamic conditions during the emplacement of tsunami sequences, together with data from grain size analysis, are presented. The value of chemical proxies as indicators of saltwater inundation, associated marine shell and/or coral, high-energy depositional environment, and possible contamination, is demonstrated and issues of preservation addressed. We also provide new findings from detailed studies of heavy minerals.

New information gathered during the UNESCO — International Oceanographic Commission (IOC) International Tsunami Survey of fine onshore sediments following the 2009 South Pacific Tsunami is presented, and includes grain size, chemical, diatom and foraminifera data. The tsunami deposit varied, ranging from fining-upward sand layers to thin sand layers overlain by a thick layer of organic debris and/or a mud cap. Grain size characteristics, chemical data and microfossil assemblages provide evidence for marine inundation from near shore, and changes in flow dynamics during the tsunami.

Contents

1. Introduction . . . 108
2. Proxies . . . 108
 2.1. Grain size characteristics . . . 108
 2.2. The magnetic fabric of tsunami deposits (Anisotropy of Magnetic Susceptibility — AMS) . . . 108
  2.2.1. Analytical procedures . . . 108
  2.2.2. Application to 2004 IOT deposits, Banda Aceh, Indonesia (Wassmer et al., 2010) . . . 109
 2.3. Heavy minerals . . . 111
 2.4. The macrobiology of tsunami deposits . . . 111
  2.4.1. Macropalaeontology . . . 112
  2.4.2. Micropalaeontology . . . 112
 2.5. Chemistry . . . 113
3. Some characteristics of the 2009 South Pacific Tsunami deposits in Samoa . . . 113
 3.1. Methods . . . 113
  3.1.1. Field . . . 113
  3.1.2. Laboratory analyses . . . 114
 3.2. Results . . . 114
  3.2.1. Ponded water . . . 114
  3.2.2. Sediment . . . 114

* Corresponding author at: Australian Tsunami Research Centre and Natural Hazards Research Laboratory, School of Biological, Environmental and Earth Sciences, University of New South Wales, Sydney NSW 2052, Australia. Tel.: +61 2 9385 8921; fax: +61 2 9385 1558.
E-mail addresses: c.chague-goff@unsw.edu.au (C. Chagué-Goff), jl.schneider@epoc.u-bordeaux1.fr (J.-L. Schneider), j.goff@unsw.edu.au (J.R. Goff), dale.dh@unsw.edu.au (D. Dominey-Howes), lukestrotz@gmail.com (L. Strotz).

0012-8252/$ – see front matter © 2011 Elsevier B.V. All rights reserved.
doi:10.1016/j.earscirev.2011.03.007

3.3. Discussion . . . 118
4. Revised 'toolkit' of palaeotsunami proxies . . . 120
5. Conclusions . . . 120
Acknowledgements . . . 120
References . . . 120

1. Introduction

Much has been written and argued about the diagnostic criteria or proxies of historical and palaeotsunamis, (e.g. Atwater, 1987; Dawson et al., 1988; Goff et al., 2001; Dominey-Howes et al., 2006; Dawson and Stewart, 2007; Kortekaas and Dawson, 2007; Morton et al., 2007; Bridge, 2008; Dawson et al., 2008; Kelletat, 2008; Morton et al., 2008; Switzer and Jones, 2008; Goff et al., 2010a, 2010b; Goto et al., 2010). Much work still remains to be done and many questions are still unanswered.

The study of modern deposits carried out during immediate post tsunami surveys provides the opportunity to refine diagnostic criteria, without the uncertainty of the generating event and preservation issues due to natural and anthropogenic disturbance. Follow-up studies, most of them carried out after the 2004 Indian Ocean Tsunami (IOT), have demonstrated some of the taphonomic issues researchers of historical and palaeo-events encounter (e.g. Szczuciński et al., 2007; McLeod et al., 2010). Although only short-term changes were addressed, these studies provided useful information for the understanding and identification of historical and palaeotsunami deposits.

It is important for researchers to examine every modern/known tsunami deposit (and landscape — i.e., geomorphology) in as much detail as possible in order to identify and characterise the impacts and nature of the event/deposit. From such work, we will develop a more sophisticated, reliable, and accepted set of diagnostic criteria. Such research will provide the underpinning data for tsunami risk assessment.

The aims of this paper are to: 1) review some of the existing 'toolkit' proxies used to identify tsunami/palaeotsunami deposits, and provide an update on rarely used proxies; 2) present new data gathered immediately after the 2009 South Pacific Tsunami (2009 SPT), on the south and south east coast of Upolu, Samoa and, 3) propose a revised 'toolkit' of tsunami sediment proxies.

2. Proxies

Refining the toolkit of proxy data is an on-going project, and it will continue to improve as our studies continue. The proxies for modern and palaeotsunami deposits can be found in Morton et al. (2007), Goff et al. (2010b), and Peters and Jaffe (2010), to cite a few, although none of the lists is exhaustive. A summary of most of the commonly used proxies as well as more detailed information on less frequently used diagnostic criteria for sandy sediments is provided below (see also Table 1). Furthermore, some of the 'common' sedimentological and stratigraphic criteria (e.g. rip-up clasts, erosional contact) not discussed in details are listed in Table 1.

2.1. Grain size characteristics

Grain size analysis and interpretation of various grain size parameters provide valuable information for both the description of the sediment and hydrodynamic interpretation of the tsunami deposits.

Several approaches have been applied to the grain size analysis of tsunami deposits. Measurements can be conducted by sieving with calibrated meshes or within settling columns for coarse deposits, whereas laser diffraction diffractometer measurements are suitable for clay to sand-sized sediments, when the coarser grains do not exceed 1 mm (Blott and Pye, 2006). Grain size data are normally expressed in either micrometres (μm) or phi (ϕ).

Statistical parameters (mean grain size, standard deviation, skewness and kurtosis) are normally calculated according to the computation method of moments of Seward-Thompson and Hails (1973). This method is particularly well adapted for obtaining grain size statistical parameters, because the whole frequency distribution is used in the computation, instead of a few selected percentiles. Mean grain size, standard deviation and skewness appear to be the most useful to the study of tsunami deposits.

Moreover, the *CM* diagram of Passega (1957, 1964) based on the fifth coarsest percentile (C95; Allen, 1971) vs. median grain size from the calculated cumulative curves provides interesting interpretations to reconstruct hydrodynamic conditions during the emplacement of a tsunami deposit (see below and Wassmer et al., 2010). The *CM* diagram suggests that transport conditions gradually change from high-energy rolling along the ground (bed load transport) to low-energy graded (leading to normal grading deposition) and uniform suspension (suspension load). The limit between bed- and suspension load (weakest currents) occurs for sediments with C95 above 500 μm.

During inundation of coastal areas by tsunami waves, sediment particles are mainly transported in suspension. The free settling of the particles through the water column, related to a decrease of the turbulence of the flow, generally forms fining-upward depositional sequences. Grain size characteristics of the tsunami deposits reflect both the origin of the displaced sediment and hydrodynamic conditions of the sedimentation. Tsunami deposits usually display common characteristics (Sugawara et al., 2008), with normally graded sand layers related to the decrease of the hydrodynamic energy during sedimentation (e.g. Dawson et al., 1988, 1991; Shi et al., 1995; Minoura et al., 2000). Each fining-upward sequence can record the effects of individual surging tsunami waves.

Alternatively, a coarsening upwards may be indicative of the long duration time of the tsunami and its source parameters (Higman and Jaffe, 2005). Tsunamis with narrower source regions are more likely to be normally graded, and those with wider sources have more complex deposits (Higman and Jaffe, 2005). This provides a basis for distinguishing the deposits of large subduction zone earthquakes from more local tsunamis.

The thickness and mean grain size of tsunami deposits *generally* decrease landwards (e.g. Shi et al., 1995; Minoura et al., 1996, 1997; Gelfenbaum and Jaffe, 2003; Goff et al., 2004a), although it also depends upon local topography (e.g. Hori et al., 2007). Furthermore, landward coarsening deposits have also been observed (e.g. Higman and Bourgeois, 2008).

2.2. The magnetic fabric of tsunami deposits (Anisotropy of Magnetic Susceptibility — AMS)

2.2.1. Analytical procedures

In rock magnetism, the magnetic fabric is coaxial to a rock's or sediment's fabric (e.g. Borradaile, 1988; Tarling and Hrouda, 1993). The magnetic fabric of rocks and unconsolidated sediments is examined using AMS (Anisotropy of Magnetic Susceptibility). Work by Hamilton and Rees (1970) confirmed that AMS parameters are diagnostic of the primary sedimentary fabrics of natural sediments. AMS can therefore be used to obtain information on the hydrodynamic conditions of the depositional environment (Taira, 1989;

Table 1
Revised proxy toolkit to identify palaeotsunami deposits, with revised and new proxies presented in this review in bold. Note that most proxies are applicable to fine sediments.
Modified after Goff et al., 2010b.

1. Particle/grain sizes range from boulders to fine mud — palaeotsunami sediment grain sizes are source-dependent
2. Sediments generally fine inland and upwards within the deposit, although coarsening upwards sub-units can be present. Deposits generally rise in altitude inland and can extend for several kilometres inland and 10's of kilometres alongshore
3. Each wave *can* form a distinct sedimentary unit and/or there may be laminated sub-units
4. Distinct upper and lower sub-units representing runup and backwash can sometimes be identified
5. Lower contact is unconformable or erosional — infilling of microtopography is visible in more recent deposits
6. Can contain intraclasts (rip-up clasts) of reworked (natural and anthropogenic) material
7. Can be associated with loading structures at base of deposit
8. **Measurement of anisotropy magnetic susceptibility (AMS) combined with grain size analysis provides information on hydrodynamic conditions 'typical' during tsunami deposition. Essential when no sedimentary structures are visible.**
9. **Heavy mineral laminations often present but source-dependent — normally near base of unit/sub-unit but not always. Composition and vertical distribution of heavy mineral assemblage recommended (e.g. often more micas at the top of the deposits),**
10. Generally associated with an increase in abundance of marine to brackish diatoms — generally a greater percentage of reworked terrestrial diatoms near the upper part of the deposit. Large number of broken valves often observed, reflecting turbulent flows. Variations in diatom affinities often indicative of source areas and magnitude of event.
11. Marked changes in foraminifera (and other marine microfossils) assemblages. Deeper water species may be introduced and/or increase in foraminifera abundance and breakage of tests. Composition relates to source (near-shore vs. offshore). Foraminifera size tends to vary with grain size
12. Pollen concentrations are often lower (diluted) in the deposit because of the marine origin and/or includes high percentage of coastal pollen (e.g. mangroves). Changes in pollen above deposit due to vegetation change associated with saltwater flooding.
13. **Increases in elemental concentrations of sodium, sulphur, chlorine (palaeosalinity indicators, including element ratios), calcium, strontium, magnesium (shell, shell hash, and coral), titanium, zirconium (associated with heavy mineral laminae if present) occur in tsunami deposits relative to under- and overlying sediments. Indicates saltwater inundation, and/or high marine shell/coral content, and/or high energy environment (heavy minerals, source-dependent). Preservation issues to be considered in particular for salt (downward leaching), but uptake and preservation in wetlands/soils.**
14. **Possible contamination by heavy metals and metalloids (source-dependent, inc. water depth source)**
15. Geochemical (saltwater signature) and microfossil evidence often extends further inland than landward maximum extent of sedimentary deposit
16. Individual shells and shell-rich units are often present (shells are often articulated and can be water-worn). Often more intact shells as opposed to shell hash. Small, fragile shells and shellfish can be found near the upper surface of more recent palaeotsunami deposits
17. Often associated with buried vascular plant material and/or buried soil and/or skeletal (human/animal) remains
18. Shell, wood and less dense debris often found "rafted" near top of sequence.
19. Often associated with archaeological remains (e.g. middens) and/or oral record. In many cases coastal occupation layers are often separated or extensively reworked at several sites along coastline
20. Known local or distant tsunamigenic sources can be postulated or identified
21. Geomorphology indicates tsunami inundation (e.g. an altered dune geomorphology, evidence of either uplift or subsidence)

Tarling and Hrouda, 1993), and transport direction of the sediments during their emplacement (e.g. Rees, 1965; Hamilton and Rees, 1970; Liu et al., 2001).

Sediment samples are usually collected in soft sediment in 2 cm^3 non-magnetic plastic boxes. For tsunami deposits, samples are normally collected along vertical trench sections (see Wassmer et al., 2010, for details), although cores can also be used (Tarling and Hrouda, 1993).

Measurements of AMS are obtained with a capacity bridge. Each sample is analysed in 15 directions to determine the magnitude and directions of the maximum, intermediate, and minimum AMS axes. The geometry of the triaxial AMS ellipsoid (e.g. Tarling and Hrouda, 1993) can be reconstructed by means of its principal eigenvectors K_{max}, K_{int} and K_{min} representing the maximum, intermediate and minimum susceptibility axes, respectively. The maximum susceptibility axis, K_{max}, is generally parallel to the mean long axis of the constituent particles and therefore to the transport direction. The AMS parameters are calculated for each sample following Ellwood et al. (1988) and Tarling and Hrouda (1993). The most important parameters are the magnetic foliation ($F = K_{int}/K_{min}$), the magnetic lineation ($L = K_{max}/K_{int}$), the shape parameter (T), the degree of anisotropy (P_j), and the alignment parameter (F_S), which allow the reconstruction of the characteristics of the AMS ellipsoids and the evaluation of the relationship between depositional processes and magnetic fabric (see Wassmer et al., 2010, for details).

The magnetic fabric is characterised by the magnetic foliation (oblate) and the magnetic lineation (prolate), and is related to the conditions in the sedimentary environment. In subaqueous sediments, the orientation of magnetic grains depends on the intensity of the bottom currents and F_S increases with their strength (e.g. Park et al., 2000). Studies of experimentally deposited sediment magnetic fabric indicate that the magnetic grains are mainly oriented parallel or close to the bedding plane, with their longer axes (i.e. K_{max}) parallel to the flow direction and with an imbrication, when existing, dipping upstream (e.g. Rees, 1965; Taira, 1989). It is necessary to normalise AMS data with grain size data.

2.2.2. Application to 2004 IOT deposits, Banda Aceh, Indonesia (Wassmer et al., 2010)

Tsunami deposits were preserved in shallow lagoons flooded by successive waves but without significant backwash between each inundation. Consequently, the lagoons were progressively infilled by sediment during the tsunami.

The deposits ranged from 2 to 80 cm thick and consisted of a succession of several cm-thick fining upward sequences with coarse sand at the base to silt at the top, forming multiple-bed deposits. Each sequence was interpreted as the deposit resulting from an individual wave (Wassmer et al., 2007).

An example of the magnetic fabric of a tsunami deposit is shown in Fig. 1, which combines grain size and AMS data. The mean bulk volume susceptibilities K_{mean} are relatively high (3.2 to 5.8×10^{-3} SI) due to the presence of ferro- (oxide-coated quartz grains) and paramagnetic minerals (amphibole and biotite) in the sediment. Values of the lineation (L), foliation (F), shape parameter (T), corrected degree of anisotropy (P_j) and alignment parameter (F_S) indicate that the AMS ellipsoids are mainly oblate. The imbrication angles of the ellipsoids are less than 20°. Values vary with lithologic changes, the coarser the sediment, the higher the lineation (Fig. 1B). Lineation is highest at the top of the basal rip-up clast-rich sandy layer, whereas foliation and shape parameters increase toward the top, independent of grain size. F_S values are highest in the reworked tsunami sediments near the surface (Wassmer et al., 2010).

Vertical variations of magnetic lineation indicate fluctuations in bed load transport during the deposition of successive sequences (i.e. during the arrival of each successive wave), whereas the lineation values generally vary with grain size. The higher lineation values in the basal layer suggest that basal shearing and traction processes were more efficient during the passage of the first wave. For later waves, the increase of the magnetic foliation and the oblate shape of the AMS ellipsoids (T) indicate that settling processes became dominant, and there was a reduction in the strength of the current. Vertical increases in values for F_S underline the increase of the grain alignment in the deposit caused by changes in the strength of the current during sedimentation. However, where there is an inverse relationship

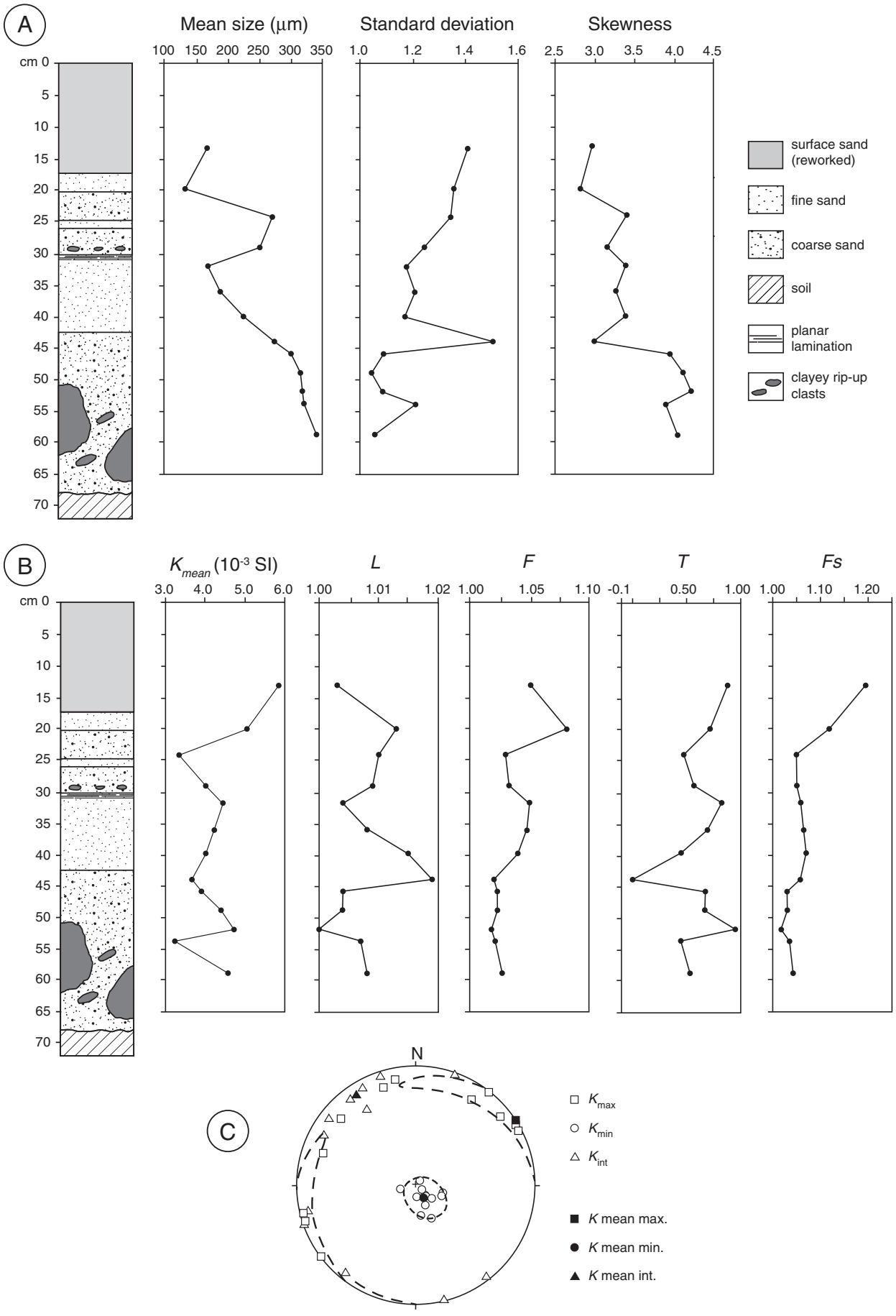

between F_S and grain size, this reflects an increase in the strength of the current when the lagoon is infilled with finer sediment as wave momentum progressively decreases during the flood. Fig. 1C is a lower hemisphere equal-area projection of the AMS data of all the samples of the presented section, with the calculated mean K_{max}. Wassmer et al. (2010) reconstructed two main directions for the K_{max} in the tsunami deposits, one parallel and the second perpendicular to the direction of waves in the area (Wassmer et al., 2007). Experimental observations on flow-controlled fabrics of sandy deposits (e.g. Allen, 1984) show that flow-parallel preferential grain orientations are related to weaker current strengths than the flow-perpendicular directions (stronger currents). Consequently, as the mean K_{max} is perpendicular to the flow direction for the section presented herein, the flood current strength was probably relatively high.

These AMS data are consistent with the decrease of the mean grain size that reflects a progressive reduction of the current strength within the superimposed sequences of the tsunami deposit (Fig. 1A). In the conditions of progressive reduction of the hydrodynamic energy, the standard deviation and skewness should decrease to reflect a better sorting of the sediment, but this is not the case. This contradiction is explained by the absence of efficient backwash in the sedimentation area. The arrival of successive waves on an already flooded area led to the progressive mixing of resuspended sediment with finer particles. Consequently, the sediment became progressively more mixed and is characterised by an increase of the standard deviation and a decrease in the skewness.

Finally, the most interesting correlation is between the AMS parameters and variations in the *CM* diagram. The *CM* diagram indicates rapid change in sediment transport mechanisms during each tsunami wave cycle (Fig. 2). On one hand, bed load of the particles is the major transport process for the basal layers of the deposit intervals as confirmed by magnetic lineation values. On the other hand, the settling of particles out of suspension in the top layers is also reflected by the mainly oblate shape of the AMS. Consequently, each individual sequence indicates that the mode of particle motion grades from bed- to suspension load transport during each wave cycle as proposed by Sugawara et al. (2008).

The applicability of the AMS technique is however limited by the size of the sampling box (19 mm), and thus the AMS technique can only be used for sediment layers thicker than 20 mm. Another limitation of the technique refers to poorly sorted sediments containing a large fraction of coarse volcanoclastic material, as the magnetic susceptibility of the latter can bias the susceptibility of the whole sample (Wassmer et al., 2010). Nevertheless, the AMS technique can provide essential information of the hydrodynamics conditions prevailing during a tsunami, in particular when they cannot be inferred otherwise, due to a lack of sedimentary structures (Wassmer et al., 2010).

2.3. Heavy minerals

The occurrence of heavy minerals is often reported in tsunami deposits (e.g. 1992 Nicaragua tsunami: Higman and Bourgeois, 2008; 2001 Peru tsunami: Morton et al., 2007; 2004 IOT: Babu et al., 2007; Szczuciński et al., 2006; Narayana et al., 2007; Morton et al., 2008), most commonly at the base (e.g. Morton et al., 2007) but also throughout the deposit (e.g. Higman and Bourgeois, 2008; Morton et al., 2008).

Detailed investigations of the heavy mineral assemblages are however, rare (Switzer et al., 2005; Babu et al., 2007; Jagodziński et al., 2009). Switzer et al. (2005) analysed the heavy mineral composition of sand sheets of mid to late Holocene age in southeastern Australia. The assemblages were different from those in the embayment, but similar to those from the mid estuary sediments and from the inner shelf, suggesting transport by a large scale overwash event (Switzer et al., 2005).

Babu et al. (2007) compared the heavy mineral assemblages of pre- and post-2004 IOT sediments and found a higher percentage of magnetite, ilmenite, sillimanite and garnet in post-tsunami sediments. The increase of magnetite, which has a higher density than the other heavy minerals it was associated with, was attributed to the intensity of reworking during the tsunami (Babu et al., 2007). SEM analysis also revealed more precipitation-corroded features in post-tsunami heavy minerals, in particular ilmenite (Babu et al., 2007). However, the position of the heavy minerals in the deposits was not reported.

Jagodziński et al. (2009) recorded a higher concentration of micas (muscovite and biotite), at the expense of tourmaline, zircon, and the opaque heavy minerals, in 2004 IOT deposits in Thailand than in beach sediments and pre-tsunami soils. Tourmaline and zircon were generally found to be dominant over the micas and opaque heavy minerals closer to the shoreline. Higher mica concentrations occurred towards the upper part of the tsunami deposits, with mica flakes found more commonly in the finest-grained sediment samples (Jagodziński et al., 2009). This preferential distribution was attributed to different modes of deposition during a tsunami, which occurs through bed load and suspension (e.g. Dawson and Shi, 2000; Sugawara et al., 2008), as opposed to bed load only in beach sediment (Jagodziński et al., 2009), and could provide another useful proxy for identifying palaeotsunami deposits. Furthermore, the presence of micas suggested a deeper water source for the tsunami sediment (than solely beach sediments) (Jagodziński et al., 2009).

However, heavy mineral laminae have been reported in both storm and tsunami deposits (e.g. Switzer et al., 2005; Morton et al., 2007; Switzer and Jones, 2008), as they are source-dependent (Morton et al., 2007), which also explains their absence in some of the tsunami deposits, such as those of the 1993 Hokkaido-nansei-oki tsunami (Nanayama et al., 2000), the 1998 Papua New Guinea tsunami (Morton et al., 2007) , and the 2009 SPT in Samoa (Richmond et al., 2011-this issue). They are indeed more often used as proxies for high-energy environmental conditions (e.g. Goff et al., 2004b; Switzer et al., 2005; Nichol et al., 2007; Switzer and Jones, 2008; Goff et al., 2010c), and while they can provide clues about the origin and depth of the wave(s), they are more likely to provide useful information when used in conjunction with other proxies.

2.4. The macrobiology of tsunami deposits

Dead fish are often reported strewn across the landscape following modern tsunamis (e.g. Lander et al., 2003; Dominey-Howes and Thaman, 2009), and other marine fauna have also been found onshore following tsunami inundation. During the 2004 IOT an Indo-Pacific Humpback dolphin (*Sousa chinensis*) was washed 1400 m inland over a 4–5 m high embankment at Phuket and a shark was stranded in a hotel swimming pool near Khao Lak, Thailand (Goff and Chagué-Goff, 2009). Sea turtles were also found washed up in ponds kilometres inland in SE Sri Lanka (Goff and Chagué-Goff, 2009). Following the 2009 SPT, sharks, rays and at least two dead dolphins were reported

Fig. 1. Sedimentological log, grain size and AMS data of a tsunami deposit in a breeding pond in the Kajhu Perumnas area (Wassmer et al., 2010). The sediment at the top of the deposit has been partially reworked by post-tsunami sedimentary agents (first 17 cm). A. Graphic representation of grain size (mean grain size in μm; standard deviation; and skewness). B. AMS data (K_{mean}: mean bulk volume susceptibility in 10^{-3} SI units; *L*: magnetic lineation; *F*: magnetic foliation; *T*: shape parameter; F_S: alignment parameter). C. Synthetic diagram of the equal-areas, lower hemisphere projections of the principal AMS tensor axes of the samples of the studied section. Mean K_{max} plots indicate the main transport directions. Confidence cones are reported for K_{max} and K_{min} projections.

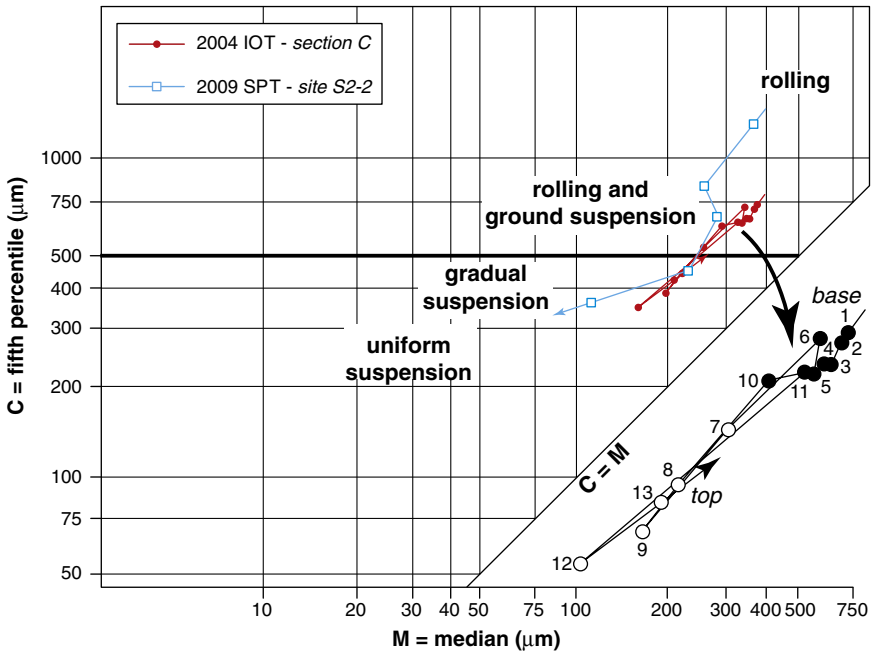

Fig. 2. *CM* diagram for the deposits of the section from Sumatra presented in Fig. 1 (red circles) (Wassmer et al., 2010), as well as for the deposits of site S2-2 from Samoa (blue squares, with arrow indicating top of sequence). M: median in µm; C: fifth percentile (C95) in µm. Enlarged diagram (Sumatra section): samples from basal (black circles) and upper (open circles) layers of the deposit intervals. Numbers (from base to top) refer to the samples along the section.

stranded inland on Upolu, as well as 51 turtles, most of which were subsequently released (Dominey-Howes and Thaman, 2009). Halimeda clusters, seaweed, shells, coral debris and fresh coral heads, in particular *Porites* spp., and some *Pavona* heads, along with smaller fragments of branching corals (*Acropora* spp.) were also found inland by various members of the survey team (Dominey-Howes and Thaman, 2009; Richmond et al., 2011-this issue).

2.4.1. Macropalaeontology

Macrofossil remains are seldom preserved within tsunami deposits, probably due to erosion, human or other animal scavenging, or other natural or anthropogenic processes. In Wellington, New Zealand, there were historical reports of a whale skeleton found about 50 m above the high water mark, and whose existence was tentatively attributed to a tsunami (Goff and Chagué-Goff, 2009), although unfortunately the whale skeleton was destroyed to make way for a residential sub-division. Intact fish skeletons were however, found in a probable 15th century palaeotsunami deposit on the west coast of the North Island, New Zealand (Cassels, 1979). Shells and shell hash are the most commonly reported macrofossils in historical and palaeotsunamis, providing another clue to the origin of the deposit (e.g. Goff et al., 2000; Nichol et al., 2007).

2.4.2. Micropalaeontology

Diatoms (e.g. Hemphill-Haley, 1996; Chagué-Goff et al., 2002; Dawson, 2007; Kokociński et al., 2009; Sawai et al., 2009) and foraminifera (e.g. Dominey-Howes et al., 1998; Hawkes et al., 2007; Kortekaas and Dawson, 2007; Dahanayake and Kulasena, 2008; Mamo et al., 2009) or both (e.g. Williams and Hutchinson, 2000; Abrantes et al., 2005; Nichol et al., 2007; Goff et al., 2010c) are the most commonly used microfossils in the identification of tsunami deposits.

2.4.2.1. Diatoms. Diatoms are unicellular microscopic algae that secrete a silt-sized frustule (valve or shell). Benthic diatom assemblages provide information on the origin and the sediment source they are associated with (e.g. Sawai et al., 2009 and references therein). Their vertical distribution in the tsunami sediments also provides information about the changes in flow conditions during the tsunami (e.g. Sawai et al., 2009). Furthermore, they can help pinpoint the landward extent of seawater inundation, beyond the area of sand distribution (e.g. Hemphill-Haley, 1996).

The vertical distribution of diatom assemblages can vary from predominantly unbroken beach and subtidal species near the base to marine planktonic species in the middle and a mix of freshwater, brackish, and marine species near the top (Sawai et al., 2009). This is consistent with changes in current velocities during inundation with the entrained freshwater, brackish, and marine species settling out with mud and organic material between waves. Sawai et al. (2009) found low numbers of broken frustules near the base as a result of rapid entrainment and deposition, with more breakage towards the upper surface associated with abrasion in the turbulent current before deposition, as also observed by Dawson (2007). Similar variations in diatom assemblage and frustule preservation are reported for palaeotsunami deposits on Futuna Island, Wallis and Futuna (Goff et al., 2011-this issue).

Preservation of diatom frustules might be limited, in particular in tropical climates, as reported by Jankaew et al. (2008), while diatom valves appear to be better preserved in mid-latitudes (e.g. Hemphill-Haley, 1996). Faster decay processes might be linked to the higher temperature in the Tropics, as shown by Kamatani (1982), who demonstrated a positive relationship between temperature and chemical dissolution of diatom valves.

2.4.2.2. Foraminifera. Foraminifera are single celled, heterotrophic protists, with many possessing a mineralised test (shell). Like diatoms, due to their small size, abundant incidence, high preservation potential within the sediment record and distinctly diagnostic shape, they are valuable stratigraphic, palaeoecological and palaeoenvironmental tools for statistical and systematic analysis and environmental reconstruction (e.g. Loeblich and Tappan, 1987; Hayward et al., 1999; Sen Gupta, 1999). Changes in assemblage composition within a sedimentary sequence are indicative of changes in marine

environmental conditions and species with restricted environmental niches are instrumental in palaeogeographic analysis and palaeoenvironmental reconstruction.

Information about the composition of foraminifera assemblages within tsunami deposits might tell us something about the depth of water from which the sediments were entrained, or their distance of transport before deposition (Uchida et al., 2010). Information about the preservation and taphonomy (environmental conditions that directly affect the preservation of fossilised remains) of individual tests might reveal something of the nature of flow velocity, turbidity, abrasion and post depositional environmental processes. Lastly, dating individual foraminifera tests contained within the tsunami deposit has the potential (depending on test wall composition and the dating methods used) to provide robust and very well constrained dates (and chronologies) for tsunami sediments where other techniques may prove problematic or are limited by available datable material (see Mamo et al., 2009 for a review), as long as the tests are preserved. As for diatoms, preservation of foraminifera tests can be problematic, as shown by Yawsangratt and al. (in press), who reported many partly or completely dissolved carbonate foraminifera tests five years after the 2004 IOT in Thailand.

2.4.2.3. Pollen and other microfossils. Pollen, dinoflagellates, silicoflagellates, radiolarians, and nannoliths are more rarely used as proxies (e.g. Chagué-Goff et al., 2002; Dahanayake and Kulasena, 2008; Goff et al., 2010c; Paris et al., 2010), although pollen is increasingly used as indicator of ecological impact of tsunamis (e.g. Hughes and Mathewes, 2003; Smith et al., 2004) and is also often used as a biochronological marker (e.g. Goff et al., 2010c). Ostracods represent another indicator of salinity change and water depth. Changes in local assemblages, population density, species diversity, age population structure as well as their taphonomic characteristics make them robust indicators in studies of both recent and palaeotsunamis (e.g. Hussain et al., 2010 and see Ruiz et al., 2010 for a review).

2.5. Chemistry

Chemical signatures are ones of the forgotten proxies (Chagué-Goff, 2010). They are only rarely used to help identify historical and palaeotsunami deposits and they are often omitted from lists of diagnostic criteria. Most of the chemical signatures provide evidence of a marine incursion (e.g. saltwater: sodium, chlorine, sulphur; shell material: calcium, strontium), while others are indicative of a high energy depositional environment (e.g. titanium, zirconium, in association with heavy mineral laminae) (see Chagué-Goff, 2010 for a review). However, as reported with other proxies, the uptake and preservation of chemical signatures vary with environmental conditions and the depositional setting, thus complicating the interpretation.

The usefulness of chemical proxies to help identify historical and palaeotsunamis has been demonstrated in a number of studies (e.g. Minoura and Nakaya, 1991; Minoura et al., 1994; Chagué-Goff and Goff, 1999; Chagué-Goff et al., 2002; Goff et al., 2004b, 2010a, 2010c; Schlichting and Peterson, 2006; Nichol et al., 2007, 2010). Nevertheless, it is still a new tool to be further investigated and refined.

Studies of the chemical signature of modern tsunami deposits started with the 2004 IOT (e.g. Szczuciński et al., 2005, 2006; Srinivasalu et al., 2008; Sujatha et al., 2008; McLeod et al., 2010). Not surprisingly, the 2004 IOT was found to result in soil salinisation (McLeod et al., 2010 and references therein), and increases in Na, Ka, Ca, Mg, Cl and SO_4 as a result of saltwater inundation (Szczuciński et al., 2005, 2006; Srinivasalu et al., 2008). This confirmed the interpretations of earlier work based on the chemical signatures of palaeotsunami deposits (Chagué-Goff, 2010). Contamination of tsunami sediments by heavy metals was also reported by Szczuciński et al. (2005, 2006), Srinivasalu et al. (2008) and Sujatha et al. (2008), in Thailand and India. Sujatha et al. (2008) recorded mainly fine sediments with a high proportion of clay, originating from the near-shore, and attributed the heavy metal contamination to domestic and sewage waste in the region. Szczuciński et al. (2005, 2006) and Srinivasalu et al. (2008) on the other hand recorded fine to medium sandy sediments, in Thailand and India, respectively. Szczuciński et al. (2005) reported strong positive relationships between the salt content and bioavailable metal concentrations, and inferred a litho- and/or anthropogenic origin for the heavy metals. Srinivasalu et al. (2008) found a strong association between heavy metals and Fe–Mn oxyhydroxides and attributed the contamination to major industries in the study area.

Studies carried out in years after the 2004 IOT showed that the water-soluble salts in surface sediments were strongly reduced a year after the event, due to dilution and leaching by rainfall, while acid leachable metalloids and heavy metals did not appear to have been affected by rain and were still in elevated concentrations when compared with pre-tsunami sediments (Szczuciński et al., 2007; Szczuciński, in press). McLeod et al. (2010) investigated the spatial distribution of salinity over time and reported vertical leaching of salt as well as horizontal movement by surface waters. The slow leaching was tentatively attributed to loss of functional drainage and the low relief of the affected areas (McLeod et al., 2010). Studies by both Szczuciński et al. (2007) and McLeod et al. (2010) thus suggest that chemical indicators of saltwater inundation are not always preserved in the 'tsunami layer', thus having important implications for palaeotsunami research. Furthermore, Szczuciński et al. (2007) and Szczuciński (in press) reported a coarsening of the sandy sediments, as a result of washing out of the finer particulates by rain, which is likely to negatively impact the preservation of chemical signatures in older deposits.

3. Some characteristics of the 2009 South Pacific Tsunami deposits in Samoa

A regional tsunami was generated by three near-simultaneous submarine earthquakes (M_W 8.1–M_W 8.0) along the northern Tongan Trench on 29 September 2009, causing severe impacts to Samoa, American Samoa and Tonga (Beavan et al., 2010; Lay et al., 2010), and also affecting Wallis and Futuna, as well as numerous islands in the central South Pacific (Lamarche et al., 2010; Okal et al., 2010).

Fieldwork was carried out under the auspices of the UNESCO — International Oceanographic Commission (IOC) International Post-Tsunami Survey Team (ITST) between 16 and 24 October 2009, and results presented below were those gathered on the south and east coast of Upolu, Samoa. One of the aims of the present study was to assess the impact of the tsunami on sediment chemistry. Here, we not only investigated surface sediments, but also the chemistry of the complete sediment column of the tsunami deposit. This is the first time that this has been done during an ITST study. Furthermore, characteristics of microfossil assemblages (foraminifera and diatoms) were used to gain additional information about the source of the sediment and the depositional processes. The combination of chemical and micropalaeontological signatures in recent deposits provides new information to help understand similar records in palaeotsunamis. We however sampled only a limited number of fine grained sediment samples for further analysis and readers are referred to Richmond et al. (2011-this issue) and Jaffe et al. (2011-this issue) for more detailed geological data and sedimentological characteristics of fine on-shore sediment deposits, and Etienne et al. (2011-this issue) for new findings on boulder deposits associated with the 2009 SPT.

3.1. Methods

3.1.1. Field

Conductivity, temperature and pH of ponded water within the landward limit of tsunami inundation, a tidal river and seawater near

the coast were measured *in situ* between 16 and 24 October 2009 at a number of sites on the south and east coast of Upolu (Fig. 3) with a TPS WP-81 pH and conductivity meter.

Samples for grain size, moisture, organic matter content, chemical and diatom analyses were collected from shallow trenches (S2-2, S2-4, S2-9, and S2-10) in an area inundated by the tsunami in Satitoa, on the east coast of Upolu. In addition, three soil samples were collected in the forest beyond the area of tsunami inundation, as indicated by a lack of salt-burned vegetation (Fig. 4).

Samples for foraminifera analysis were obtained by digging a shallow trench (WS09/T14) to expose a cross section of the deposit, and sampling 1 cm 'slices' from the tsunami sand (11 cm thick) and the underlying soil.

3.1.2. Laboratory analyses

Sediment samples were dried at 105 °C overnight to determine the moisture content and subsequently ashed at 550 °C for 4 h to determine the organic matter content (loss on ignition = LOI), following Santisteban et al. (2004). Representative sub-samples were ground with a carbide mill and then pressed into pellets for X-ray Fluorescence analysis. Data were analysed using a Panalytical PW2400 XDXRF. Grain-size analysis of most samples was determined by laser diffraction on a Malvern Mastersizer 2000, except for three samples that were dry sieved using half-phi sieves.

Samples for diatom analysis were prepared following standard techniques (e.g. Battarbee, 1986) and diatoms identified following Krammer and Lange-Bertalot (1986, 1988, 1991a, 1991b) and Witkowski et al. (2001).

Samples for foraminifera analysis were dried at room temperature (30 °C or less) and picked using an Olympus SZ60 binocular microscope. 300 specimens were picked from each sample, except in the lower part of the section, due to lack of material. The picked sediment was then weighed to determine absolute abundance values. Counts were converted to individuals per gramme and to percentages to allow easy comparison between samples.

3.2. Results

3.2.1. Ponded water

The conductivity of ponded water at sites from Safaatoa to Satitoa (Fig. 3) ranged between 370 μS cm^{-1} (freshwater) and 21.1 mS cm^{-1} (brackish) ($n = 18$) (Figs. 5 and 6A). Freshwater (<c. 800 μS cm^{-1}) was recorded in only two of the ponds, while the water in all other ponds was slightly to strongly brackish. Only two recordings were made of seawater, and the conductivity of seawater was found to be fairly low in Vaovai (29.3 mS cm^{-1}), near the mouth of a tidal river, which is likely to have resulted in mixing of seawater and freshwater, but close to the normal range near Safaatoa (44.5 mS cm^{-1}). Recording started two weeks after the 2009 SPT, and while there was no rainfall prior to the first sampling date, heavy rainfall fell on the first sampling date, 15 October.

3.2.2. Sediment

3.2.2.1. Sediment characteristics. In Satitoa, the tsunami deposit consisted of a poorly sorted light yellow medium calcareous sand fining upwards to a moderately sorted medium-fine sand, overlain by a moderately well sorted grey fine sand (Figs. 6B and 7). The contact between the yellow and grey sands was sharp, but there was no evidence for it being erosional. The yellow and grey sand sequence thinned and fined inland to a poorly sorted light yellow medium to muddy sand, displaying a sharp unconformity with the underlying orange-brown volcanic soil. Infilling of microtopography was also observed in places (see Fig. 6C and D). While the tsunami sand was exposed at the surface near the coast, it was overlain by a thin (1–3 mm) discontinuous, grey mud cap further inland. The mud cap became thicker and finer inland, reaching a maximum of 6–8 cm in shallow, topographic lows (Figs. 4 and 6C). A thick layer of organic debris (up to 12 cm in topographic lows) was observed overlying the thinning sand layer close to the forest edge. This in turn was overlain by the grey mud cap up to 2 cm thick (Fig. 6D). Mud cracks were observed in most areas, although the mud was still moist where the mud was thickest (in depressions). Laminations were also observed in some trenches near the beach (see Richmond et al., 2011-this issue), but not in the sites sampled and reported here.

The moisture and organic matter content (LOI) followed the same trend, being lowest in the basal coarse sand layer (19% moisture and 4% LOI) and highest in the organic debris (77% moisture and 51% LOI; Fig. 4). Moisture and LOI of the volcanic soil beyond the area of tsunami inundation were around 41% and 24%, respectively. Similar moisture and LOI were recorded in soil samples underlying the tsunami deposit in the topographic lows (S2-9 and S2-10), while they were much lower in the soil nearest the beach (S2-2), where sand was mixed with the soil.

3.2.2.2. Sediment chemistry. Chlorine (Cl), sulphur (S), sodium (Na) and bromine (Br) concentrations exhibited a similar distribution, and were highest in the organic debris (S2-10), with up to 5.9% Cl, 2.2% S

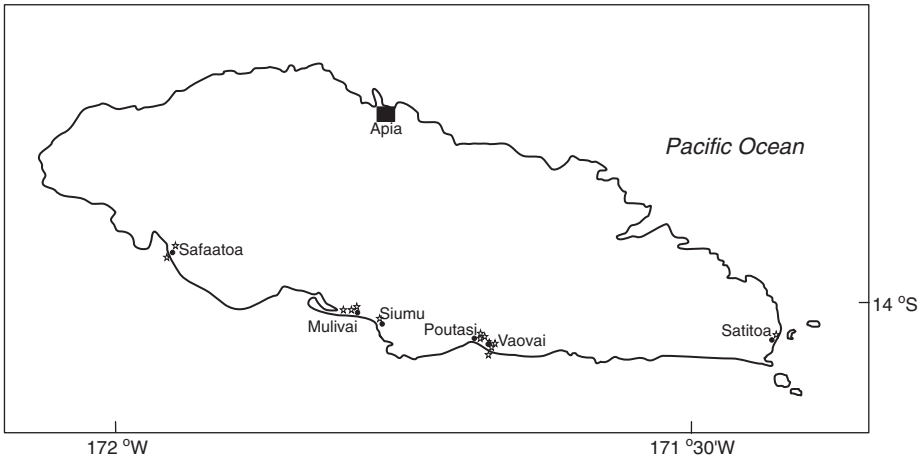

Fig. 3. Map of Upolu Island, Samoa, with locations of sampling of ponded water (☆) and sediment sampling (Satitoa). The location of the capital Apia is also shown.

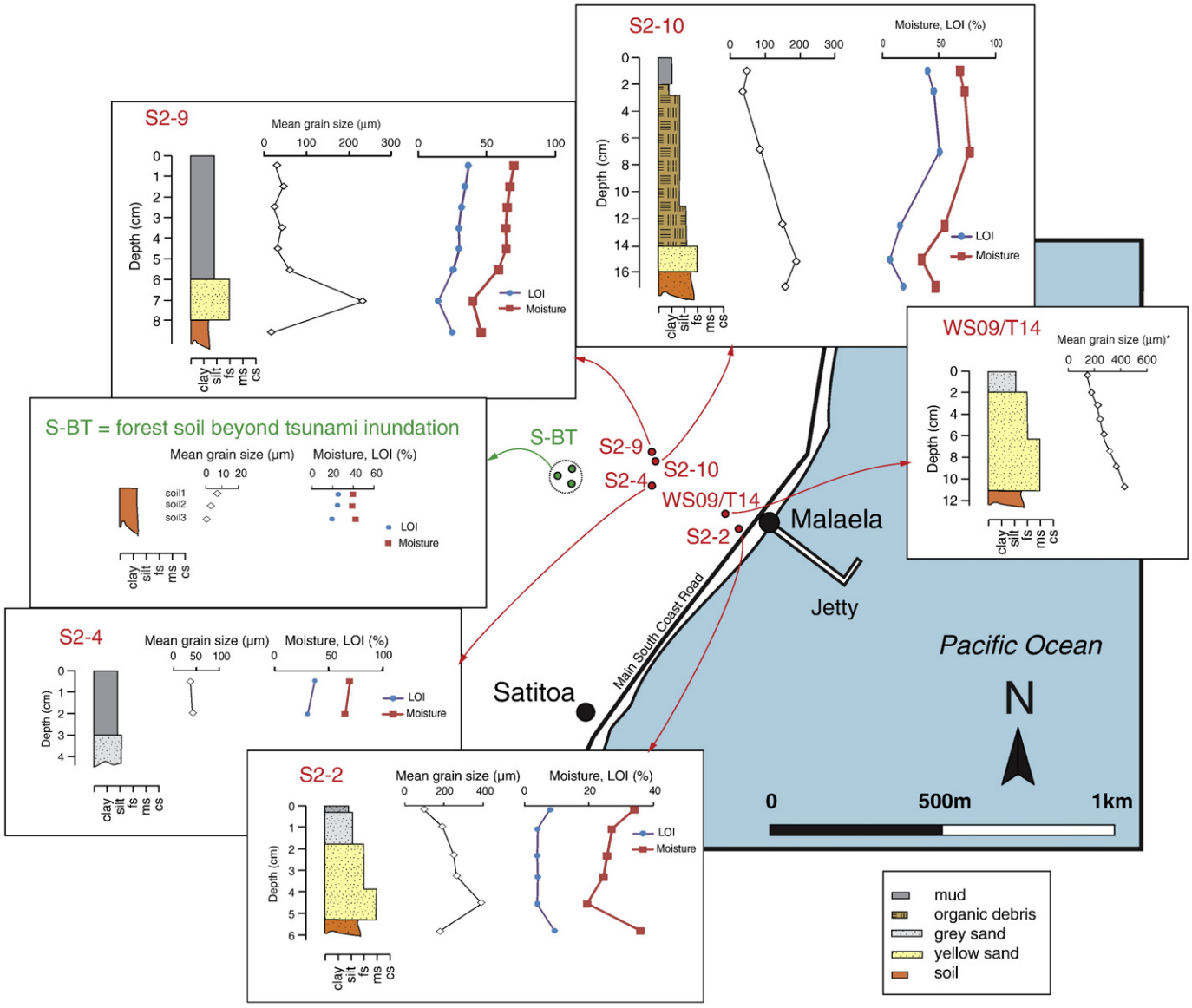

Fig. 4. Location map in Satitoa, with stratigraphy, mean grain size, moisture and organic matter (LOI) content of sites sampled. *Mean grain size data for site WS09/T14 were obtained from a neighbouring trench (25 m away).

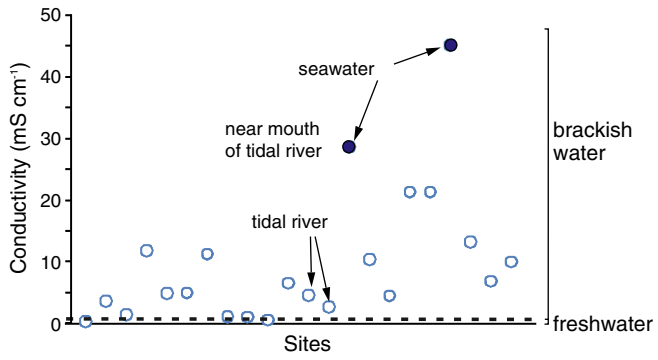

Fig. 5. Conductivity (in mS cm^{-1}) of ponded water at sites on south and south east coast of Upolu, tidal river in Vaovai and seawater. The dashed line indicates the limit between freshwater (≤c. 0.8 mS cm^{-1}) and brackish water (≥c. 0.8 mS cm^{-1}). Note 1000 µS cm^{-1} = 1 mS cm^{-1}.

and 4.2% Na (Fig. 8). They were also high in the mud cap, with concentrations of up to 1.7% S, 1.6% Cl and 1.6% Na (Figs. 7 and 8), while they were much lower in the sandy layers (0.04 to 0.1% Cl; 0.07 to 0.3% S). Cl, S, Na and Br distribution thus appeared to be both dependent on the organic matter content and the influence of saltwater inundation. These elements are in higher concentration in seawater than freshwater, and are thus often used as indicators of salinity in depositional environments (Chagué-Goff, 2010). Salt crusts (NaCl) were also observed at the surface of many wetlands on the south coast of Upolu, more than two weeks after the tsunami, despite the rainfall. It is also interesting to note that salt residues were reported in a number of areas beyond the landward limit of sediment deposition, thus providing another indicator of the limit of tsunami inundation.

The low Cl, Na and S concentrations (<0.02% Cl, <0.2% Na, and <0.4% S) in the volcanic soil beyond the area of tsunami inundation (S-BT), despite the high organic content, are a clear indication that no saltwater flooding occurred and provide background levels of these elements in non-affected soils. The relatively high Cl and Na

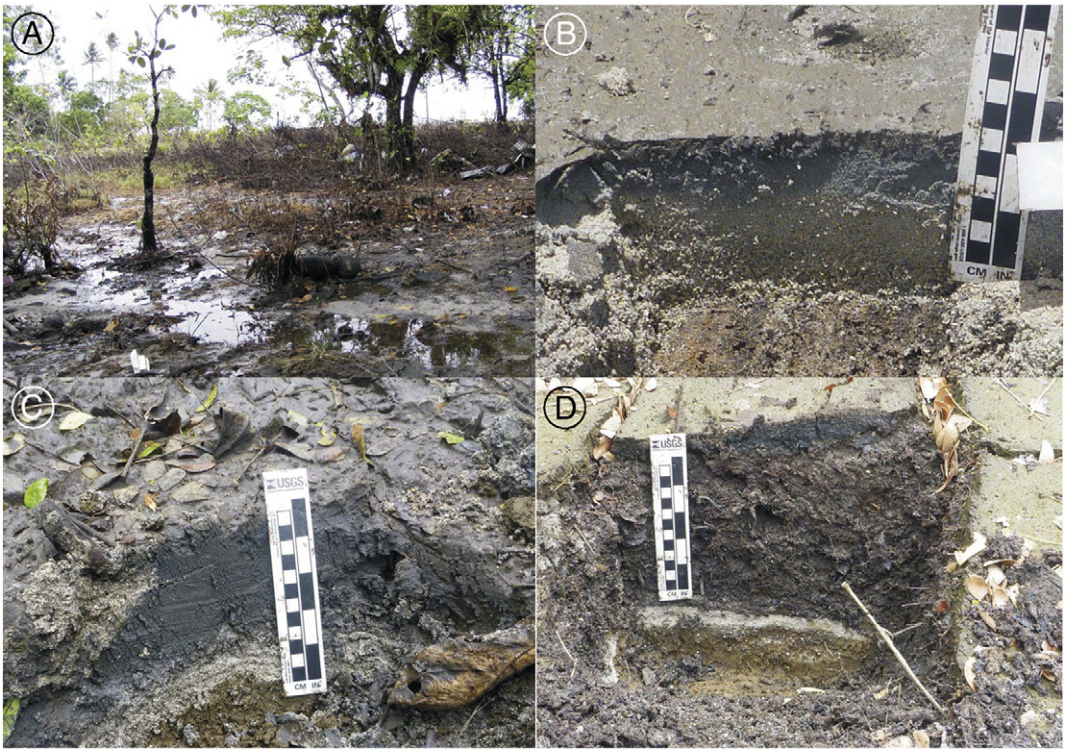

Fig. 6. A. Ponded water and salt-burned vegetation in Poutasi. B. Tsunami deposit consisting of fining-upward sand (yellow and grey) overlain by thin mud cap (site S2-2; see Fig. 4). C. Tsunami deposit consisting of thin yellow sand overlain by an 8 cm thick mud cap, observed in topographic low (e.g. site S2-9; see Fig. 4). D. Tsunami deposit consisting of thin yellow sand overlain by thick layer of organic debris and thin mud cap, observed in topographic low near edge of forest (site S2-10; see Fig. 4).

concentrations (c. 0.8% Cl and Na) in the soil underlying the tsunami deposit at site S2-9 on the other hand, suggest that some seawater had leached downward.

Calcium (Ca) and strontium (Sr) concentrations exhibited a strong positive relationship, and were generally highest in the calcareous sand (Figs. 7 and 8), followed by mud and organic debris, reflecting

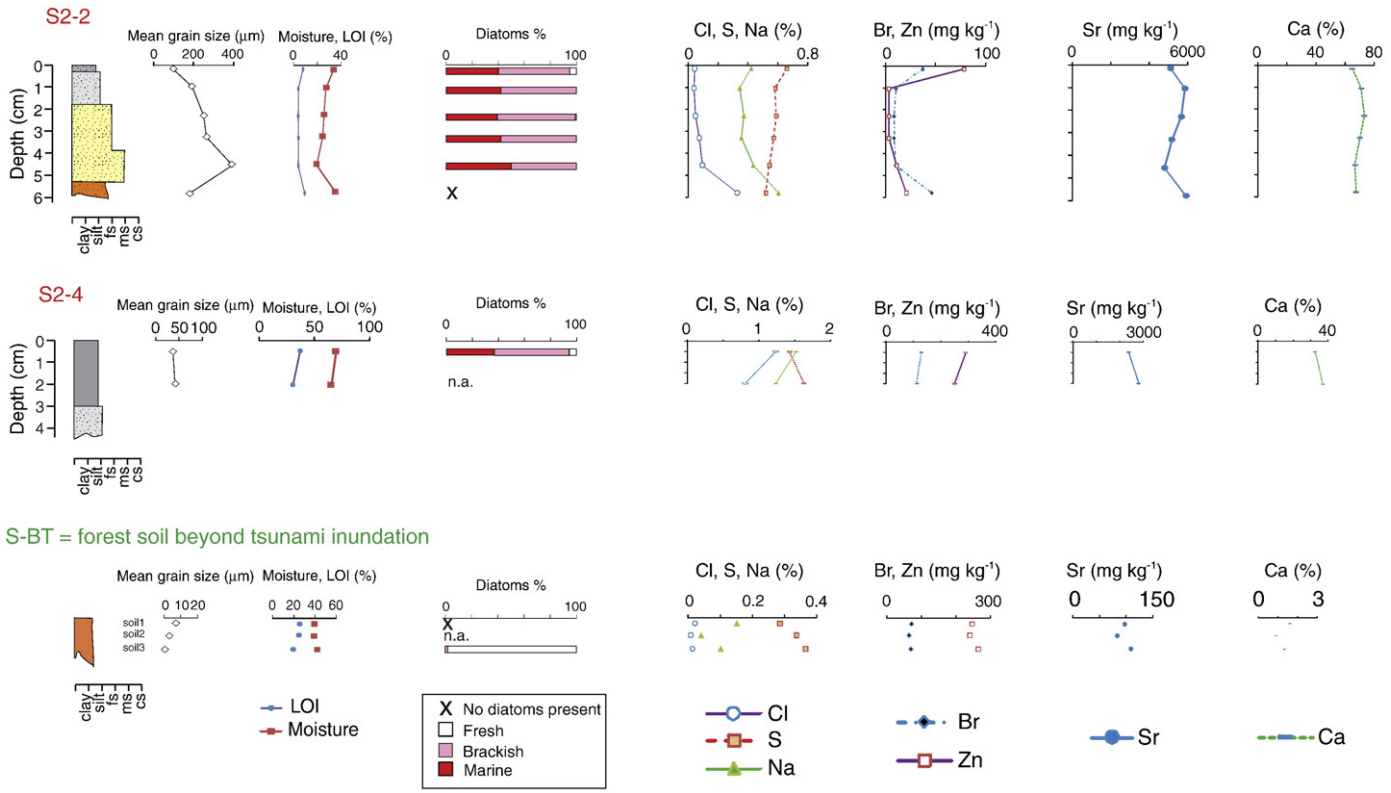

Fig. 7. Stratigraphy, mean grain size, moisture and organic matter (LOI) content, diatom data and chemical composition for trenches S2-2, S2-4 (mud cap only) and S-BT (soil beyond area of tsunami inundation). Classification of diatom data according to salinity preference. Data for S-BT are presented for each of the three samples and are not depth-dependent.

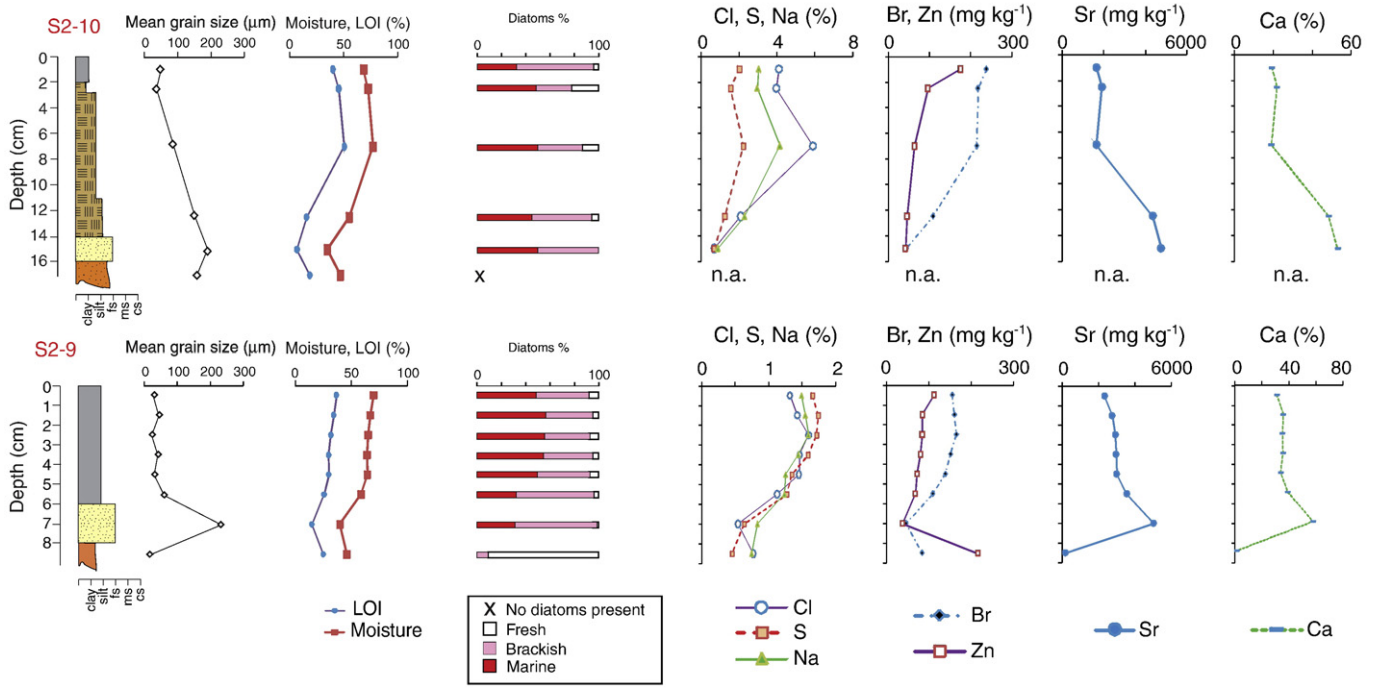

Fig. 8. Stratigraphy, mean grain size, moisture and organic matter (LOI) content, diatom data and chemical composition for trenches S2-9 and S2-10. Classification of diatom data according to salinity preference.

the contribution of shell and coral material to the tsunami deposits. Sr and Ca concentrations on the other hand were one order of magnitude lower in the S-BT and in the soil underlying the tsunami deposit in a topographic low (S2-9). Mixing of calcareous sand with the soil near the beach (S2-2) is reflected in high Sr and Ca concentrations and higher mean grain size (Fig. 7).

Zinc (Zn) concentrations were higher in the mud cap than in the sand layer (68–292 mg kg^{-1} and 3–42 mg kg^{-1}, respectively) (Figs. 7 and 8), and ranged between 210 and 265 mg kg^{-1} in the soil beyond the area of tsunami inundation and in topographic lows. Similarly, lead (Pb) and cadmium (Cd) concentrations in the mud cap samples were in the same range as in the volcanic soil ($\leq$14 mg kg^{-1} Pb and $\leq$20 mg kg^{-1} Cd; data not shown).

3.2.2.3. Microfossils. Between 208 and 351 diatom frustules were counted in each sample, except in the soil samples (no diatoms or 38–53 frustules). When present, diatoms in soil samples, both beyond the area of tsunami inundation and below the tsunami deposits, were predominantly benthic freshwater (e.g. *Navicula seminulum* and *Navicula spp.*), with a few euryhaline species (one out of 38 diatoms in S-BT, or five out of 53 in a topographic low at S2-9). Diatom assemblages in the sandy component of the tsunami deposit at the three sites (S2-2, S2-9 and S2-10) were composed entirely of benthic marine (e.g. *Amphora marina, Amphora helenensis, Nitzschia persuadens, Navicula ramossina, Fallacia niella)* and brackish (e.g. *Amphora coffeaeformis, Amphora delicatissima, Amphora exigua, Fallacia forcipata, Nitzschia valdestriata, Nitzschia coarctata)* taxa (Figs. 7 and 8). Few freshwater taxa were found in the sandy layers (<1% of the total diatom assemblage).

Diatom assemblages in the mud cap and the layer of organic debris on the other hand, included not only marine and brackish, but also freshwater (e.g. *N. seminulum, Diadesmis contenta, Rhopalodia acuminatum, Bacillaria paxillifer)* taxa (Figs. 7 and 8), with 4–8% freshwater species in the mud cap (at either site). The percentage of freshwater taxa in the layer of organic debris increased from 6% above the sand to 24% near the surface underneath the mud cap (6% freshwater taxa) (Fig. 8).

Foraminifera assemblages (Plate 1) were recovered from the 12 examined horizons in the small trench, and contained significant numbers (c. 58%) of specimens often referred to as the 'larger foraminifera' (Hallock, 1985), called as such because of their larger size (between 0.5 and 20 mm) compared to the majority of foraminifera species. The remainder of the recovered fauna was composed of smaller benthic taxa that either live at the sediment/water interface or are shallow infaunal.

Relative abundance varied throughout the section, with a steady upward increase in the relative abundance of smaller benthic taxa, mainly representatives of the genus *Quinqueloculina*, at the expense of the 'larger' taxa (Fig. 9). The upper and finer part of the section contained a larger proportion of smaller benthic taxa, 'Larger' foraminifera present in the upper part of the deposit (only 5%) were more diminutive examples of the relevant taxon. The proportion of 'larger' foraminifera increased with depth, and overall test sizes of both larger foraminifera and smaller benthic taxa were also larger. The absolute abundance of foraminifera tests (tests/gramme dry weight sediment) ranged from 8.82 (near the base of the section) to 174.63 tests/gramme (towards the top of the section), and was inversely proportional to grain size (Fig. 9).

The taphonomic grade of foraminifera tests was relatively consistent throughout the tsunami deposit. Tests of smaller benthic forms were often broken (with up to 40% of the test missing) but there was little evidence of any alteration (abrasion and dissolution) of the test surface. 'Larger' taxa, such as the robust tests of *Baculogypsina sphaerulata* (Parker and Jones) and *Amphistegina lobifera* Larsen, exhibited similar levels of breakage but were also partially abraded, probably as a result of pre-tsunami taphonomic effects. 'Larger' foraminifera all live epiphytically, usually attached to macroalgae, and they only detach from this macroalgal substrate upon death, becoming incorporated into the sediment (e.g. Debenay and Payri, 2010). Thus, all larger foraminifera tests found in the sediment represent the remains of dead individuals. The taphonomic grade of

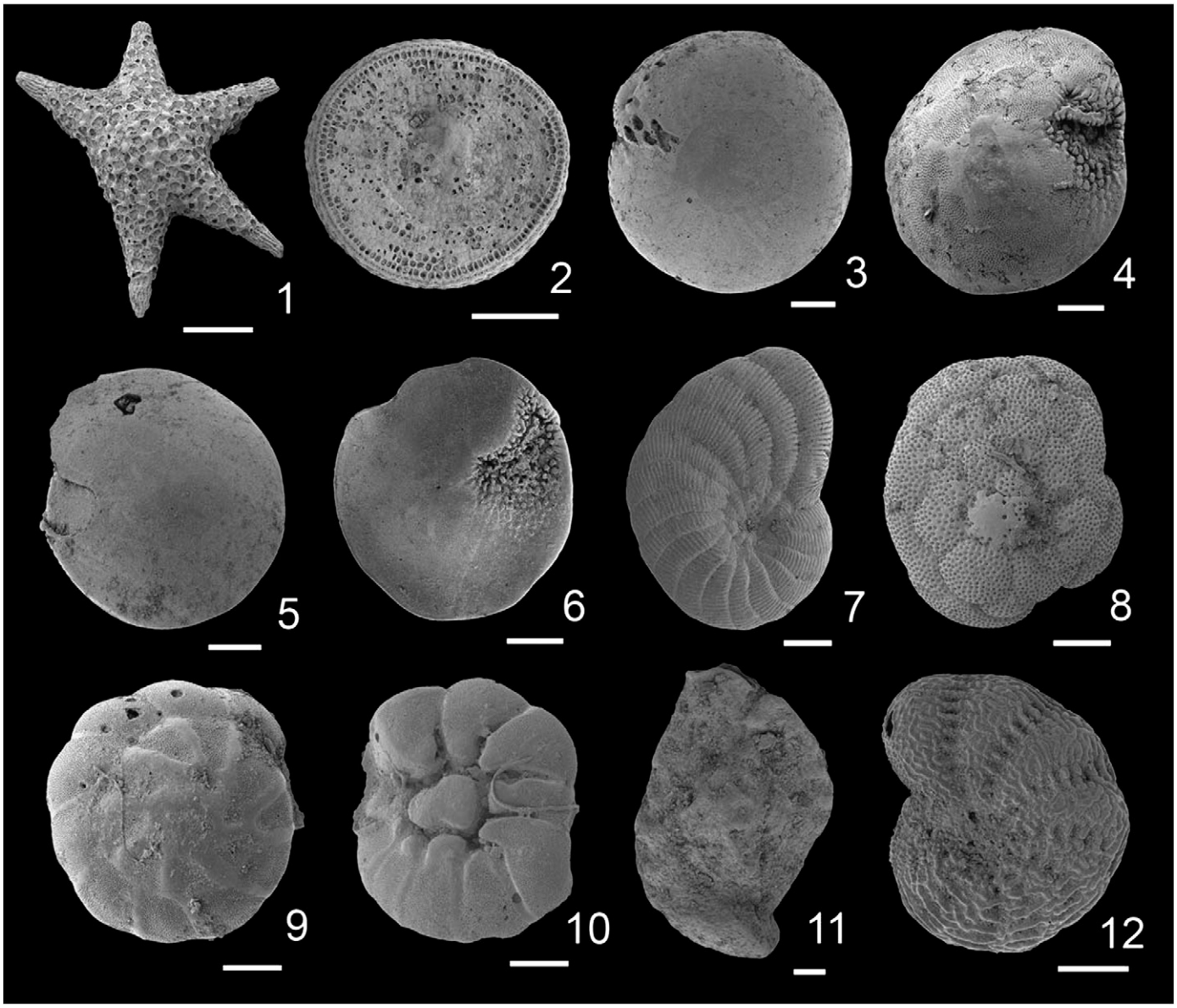

Plate 1. Foraminifera recovered from the tsunami deposit in Satitoa (site SW09/T14). 1. *Baculogypsina sphaerulata* (Parker and Jones 1860), WS09/T14 1–2 cm (scale = 500 μm); 2. *Marginopora vertebralis* Quoy and Gaimard 1830, WS09/T14 2–3 cm (scale = 500 μm); 3–4. *Amphistegina lobifera* Larsen 1976, 3 from WS09/T14 5–6 cm, 4 from WS09/T14 2–3 cm (scale for 3 = 200 μm; scale for 4 = 100 μm); 5–6. *Amphistegina lessonii* d'Orbigny 1826, 5 from WS09/T14 2–3 cm, 6 from WS09/T14 5–6 cm (scale for both 5 and 6 = 200 μm); 7. *Peneroplis pertusus* (Forskal 1775), WS09/T14 2–3 cm (scale = 200 μm); 8. *Cymbaloporetta bradyi* (Cushman 1915), WS09/T14 0–1 cm (scale = 100 μm); 9–10. *Ammonia tepida* (Cushman, 1926), 9 from WS09/T14 1–2 cm, 10 from WS09/T14 2–3 cm (scale for both = 100 μm); 11. *Quinqueloculina subpolygona* Parr 1945, WS09/T14 4–5 cm (scale = 100 μm) 12. *Elphidium reticulosum* Cushman 1933, WS09/T14 5–6 cm (scale = 100 μm).

foraminifera tests recovered from the underlying soil material was much lower than that of the tests recovered from the tsunami deposit. Breakage levels were comparable but surface abrasion levels were much higher, with tests often almost indistinguishable.

3.3. Discussion

Heavy rainfall fell on 15 October 2009, on the first day water conductivity was recorded, and is likely to have contributed to dilution and leaching of ponded saltwater, as previously reported by Szczuciński et al. (2006, 2007) and McLeod et al. (2010). Nevertheless, brackish water and salt crusts were found in wetlands, both within and beyond the landward limit of sediment deposition (see also Fig. 12 in Richmond et al., 2011-this issue), as had Fritz et al. (2007), who reported salt crusts 700 m beyond the area of sediment deposition following the 2006 Java tsunami. Salt-burned vegetation (grass, shrubs, and trees; see Fig. 6A) observed within two to three weeks after the 2009 SPT provided evidence for the extent of saltwater inundation during the tsunami, even beyond the area of sediment deposition. This is in sharp contrast with the lack of salt-burned vegetation observed following Tropical Cyclone Yasi in February 2011 in north Queensland, Australia (Chagué-Goff et al., 2011), where green grass and other vegetation were found amongst boulders and within the seaward limit of the debris line (pers. observation).

This has three implications for palaeotsunami research. First, although further downward leaching of saltwater as reported by McLeod et al. (2010) is again likely to occur, studies have shown that Cl and/or Br relative maxima occurred in palaeotsunami deposits (Schlichting and Peterson, 2006; Goff et al., 2010a, 2010c; Nichol et al., 2010). This is probably due to the transformation of Cl and Br to organohalogens during peat decomposition, and resulting binding with the organic matter, although they were first deposited as salt (Chagué-Goff and Fyfe, 1996; Biester et al., 2004), thus allowing their

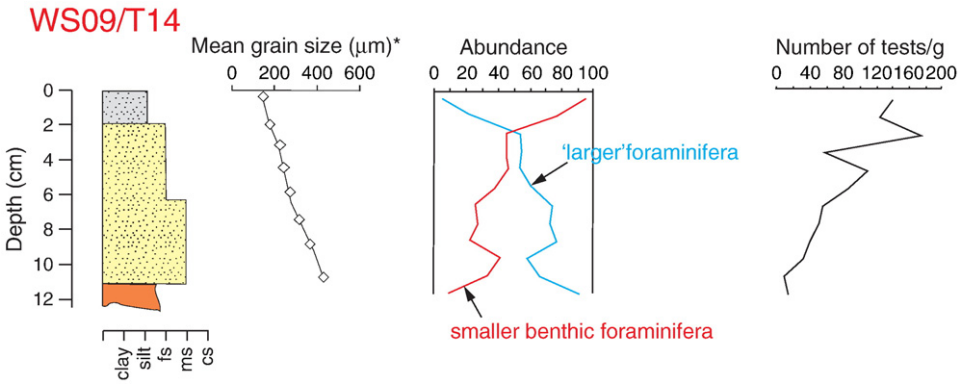

Fig. 9. Stratigraphy, mean grain size, foraminifera distribution and number of foraminifera per gramme dry weight in trench WS09/T14. *Mean grain size data were obtained from a neighbouring trench (25 m away). "Larger" foraminifera are those ranging between 0.5 and 20 mm in size, while smaller benthic foraminifera are smaller in size.

preservation in a suitable depositional environment. Second, while most researchers use the landward limit of sediment to identify the extent of past tsunamis, the chemical signature can provide a better estimate of the limit of inundation (Chagué-Goff, 2010), similar to diatoms that have been found beyond the area of tsunami inundation (Hemphill-Haley, 1996). The revised limit of inundation of past tsunamis has thus important implications for tsunami risk assessment. Furthermore, downward leaching of salt to the underlying soil, as observed at some of the sites here despite the lack of marine diatoms, and subsequent preservation with the organic matter, can help identify the limit of inundation of a tsunami, while bearing in mind the limitations due to downward leaching. Third, this may provide another proxy to distinguish between storm and tsunami deposits, with the former deposits lacking the strong marine signature, although further research is required to test this hypothesis.

Preservation of chemical signatures in coarser sediments (such as sand) is more problematic (e.g. Chagué-Goff et al., 2002; Chagué-Goff, 2010; Nichol et al., 2010), although peaks in Ca, Na, Ba and Sr, mostly attributed to the occurrence of shell and shell hash, have been reported in sandy palaeotsunami deposits (e.g. Goff et al., 2004b, 2010c; Nichol et al., 2007, 2010). Similarly, elements associated with heavy mineral laminae (e.g. titanium (Ti), zirconium (Zr)) are well preserved in sandy deposits (e.g. Goff et al., 2004b, 2010c; Nichol et al., 2007), although it is acknowledged that their occurrence is source-dependent, as inferred in Section 2.3. Sulphur on the other hand is usually better preserved in organic-rich and fine sediments, due to its affinity with organic matter (e.g. Chagué-Goff, 2010) or organic matter requirement for pyrite formation (Chagué-Goff and Goff, 1999).

Heavy metals occurred in higher concentrations in fine sediments than in the coarser sediments. However, the tsunami does not appear to have resulted in any contamination of sediments on the southeast coast of Upolu, unlike previous reports by Szczuciński et al. (2006) in Thailand, and Srinivasalu et al. (2008) and Sujatha et al. (2008) in India. This might be due to a number of reasons, such as the lack of industries in this predominantly tourist region, but also the source (water depth and distance off-shore) of the sediment deposited on-shore. It is acknowledged that the different analytical technique used in this study (XRF) might have resulted in 'dilution' of the possible contamination with the 'clean' matrix of the sediment, when compared to acid leachable concentrations reported by Szczuciński et al. (2005), Srinivasalu et al. (2008) and Sujatha et al. (2008). However, the results of this study suggest that, similar to the presence or absence of heavy mineral laminae in recent, historical and palaeotsunami deposits, heavy metal (and/or metalloid) proxies are source-dependent. Heavy metal contamination associated with palaeotsunami deposits has never been reported from New Zealand (Chagué-Goff and Goff, 1999; Goff and Chagué-Goff, 1999; Chagué-Goff et al., 2002; Goff et al., 2004b, 2010a, 2010c; Nichol et al., 2007, 2010), not because heavy metal concentrations were not determined, but because there was no contamination. It is not surprising in New Zealand, due to the lack of any industries prior to European settlement in the early-mid 1800s. It is however acknowledged that some heavy metal contamination might be found in association with historical and palaeotsunami deposits in many other countries, and this can provide another proxy for palaeotsunami deposit, in conjunction with other diagnostic criteria. Nevertheless, it might also be related to the depth and distance offshore from which the tsunami sediments originated.

The foraminifera assemblage recovered from the deposit was characteristic of a shallow water reef-flat style setting (e.g. Cushman, 1924; Hottinger et al., 1993; Parker, 2009), and was comparable to those recovered from reef-flat settings as part of previous work in the region (Cushman, 1924). Communities dominated by larger foraminifera are typical of Pacific tropical reef flat settings, where the larger foraminifera live attached to abundant epiphytes, such as seagrasses and macroalgae (Debenay and Payri, 2010). This therefore suggests that the sediment source was from near-shore. There was no evidence for a deeper water source over the reef crest (greater than 10 m), as none of the taxa consisted of the distinct forms (such as alveolinids) that occur in these settings (Ghose, 1977). Entrainment of sediment must thus have occurred in shallow water, probably no more than a few hundred metres from the shoreline. Foraminifera provided clear evidence of sorting in the deposit. Their distribution could be directly related to test size, with smaller taxa concentrated in the finer grained upper part of the deposit and larger taxa concentrated in the coarser base of the deposit. Absolute test abundance was also highest in the finer grained material in the upper section of the deposit, due to large numbers of small tests.

There was a clear distinction between the taphonomic grade of foraminifera tests from the tsunami deposit and those from the underlying sediment. The higher levels of surface alteration in the soil layer reflect transport over an extensive period of time. 'Larger taxa' have a long residence time (Resig, 2004) due to their large robust test and, as such, they are able to persist in the sediment over long time scales, whereas the smaller benthic forms are less able to survive extended taphonomic effects. As the soil layer at that particular site (WS09/T14), at close proximity to the present beach, is likely to represent former beach sands, the larger taxa in the soil represent tests that have been slowly transported near-shore by wave, tide and current action.

The fining-upward sequences and associated changes in diatom assemblages, from marine–brackish to 'chaotic' assemblages comprising marine, brackish and freshwater taxa, and foraminifera assemblages, from mostly larger to small benthic taxa, reflect the changes in flow condition during the tsunami. The lack or scarcity of freshwater diatoms in tsunami deposits, in particular in the lower

sections of the deposits, has been reported by Sawai et al. (2009) in tsunami deposits following the 2004 IOT in Thailand. This has been attributed to strong currents during the tsunami, which only allowed benthic marine diatoms attached to heavier sandy substrate to settle. The large number of freshwater diatoms associated with the finer sediments and organic debris in the upper part of the tsunami deposit is attributed to their incorporation as the turbulent tsunami currents reach further inland, eroding, transporting and redepositing terrestrial taxa picked up in the process (e.g. Dawson, 2007; Sawai et al., 2009). The association of these mixed assemblages with fine sediments in the upper part of the tsunami deposit reflects deposition due to a wanning flow in the final stages of tsunami runup (e.g. Sawai et al., 2009). This corroborates data obtained using the CM diagram, (Fig. 2; data from core S2-2), suggesting the change in sediment transport mechanism from sediment deposited at the base of the tsunami deposit to that deposited during the final stages of the tsunami.

Thus, this study illustrates that a combination of proxies, such as fining-upward sequences with distinctive changes in microfossil assemblages and a better chemical preservation toward the top (related to the finer fraction) can help identify palaeotsunami deposits and could possibly also allow for the identification of successive tsunami waves, if there were any.

4. Revised 'toolkit' of palaeotsunami proxies

The study of modern tsunami deposits during immediate post-tsunami surveys allows the refinement of the toolkit of proxies for the identification of palaeotsunami deposits, without the issues related to preservation due to natural and anthropogenic disturbance, despite the fact that any disturbance cannot be totally avoided, and rain cannot be stopped either. Here, we present a revised toolkit, based on knowledge gained following the 2004 IOT and 2009 SPT (Table 1). We have not reviewed all studies carried out following the 2004 IOT, also because we acknowledge that many data gained are site specific. We have on the other hand focussed on some rarely used proxies and new proxies. These include new findings related to heavy mineral assemblages following the 2004 IOT, the new application of anisotropy of magnetic susceptibility (AMS) in association with grain size analysis to the study of tsunami deposits following the 2004 IOT, as well as the extension and refinement of the use of chemical proxies, following both the 2004 IOT and 2009 SPT. Readers are referred to Sections 2.2 (AMS), 2.3 (Heavy minerals), 2.5 (Chemistry) and 3 (Some characteristics of the 2009 SPT deposits in Samoa) for further details on these rarely used proxies. Furthermore, we cannot emphasise enough that although it is not always practical to study every possible criterion presented in Table 1, also because some may not be relevant to the area, and/or are source-dependent, or are missing due to post-depositional changes, using newer proxies in conjunction with others that are more commonly used (e.g. grain size characteristics, stratigraphy, microfossil assemblages) is the key to success when it comes to positive identification of deposits. Nevertheless the process of refining the set of diagnostic criteria is an ongoing process and thus, the present revised toolkit is only another step towards a better toolkit.

5. Conclusions

Some of the proxies used to identify tsunami and palaeotsunami deposits were reviewed, including grain size and the macrobiology of tsunami deposits, with particular emphasis on rarely used proxies, such as heavy minerals and chemical proxies, as well as an update on a new proxy, the anisotropy of magnetic susceptibility (AMS), used following the 2004 IOT and the 2009 SPT. The vertical distribution of heavy minerals can provide information about the changes in flow dynamics, but as they are source-dependent, they may be absent from deposits. AMS can deliver information on the fabrics of tsunami deposits, a proxy of hydraulic characteristics during emplacement, as long as AMS data are associated with grain size data. AMS is sensitive enough to reconstruct the hydrodynamic conditions that prevailed during the emplacement of sequences recording the effects of individual tsunami waves. Chemical proxies provide evidence for saltwater inundation, associated coral and/or shell material, high-energy flows (heavy minerals, if present), and possible contamination associated with tsunamis. Nevertheless, like many other proxies, they are subject to taphonomic issues, which complicate the interpretation. The combination of grain size characteristics, chemical proxies and microfossil assemblages was used in the study of the 2009 SPT to provide information about the origin of the sediment, changes in flow dynamics and depositional processes during the tsunami.

Acknowledgements

We acknowledge funding support from the Australian Research Council grant DP0877572, and the support of the Samoan Government, the Samoan people and UNESCO during the UNESCO — IOC International Tsunami Survey. Faigame Sale from the Ministry of Natural Resources and Environment, Meteorology Division in Samoa is thanked for his contribution during the fieldwork survey in October 2009. XRF analysis was carried out at the Mark Wainwright Analytical Centre, University of New South Wales, while diatom analysis was undertaken by Diatoma, University of Adelaide. We would also like to acknowledge Dr Witold Szczuciński and Dr Patrick Wassmer for their constructive comments on an earlier draft of this manuscript.

References

Abrantes, F., Lebreiro, S., Rodrigues, T., Gil, I., Bartels-Jónsdóttir, H., Oliveira, P., Kissel, C., Grimalt, J.O., 2005. Shallow-marine sediment cores record climate variability and earthquake activity off Lisbon (Portugal) for the last 2000 years. Quaternary Science Reviews 24, 2477–2494.

Allen, G.P., 1971. Relationships between grain size parameter distribution and current patterns in the Gironde estuary (France). Journal of Sedimentary Petrology 41 (1), 74–88.

Allen, J.R.L., 1984. Sedimentary structures — their character and physical basis. Vol. 1. Developments in Sedimentology 30A (593 pp.).

Atwater, B., 1987. Evidence for great Holocene earthquakes along the outer coast of Washington state. Science 236, 942–944.

Babu, N., Babu, D., Das, P., 2007. Impact of tsunami on texture and mineralogy of a major placer deposit in southwest coast of India. Environmental Geology 52, 71–80.

Battarbee, R.W., 1986. Diatom analysis. In: Berglund, B.E. (Ed.), Handbook of Holocene Palaeoecology and Palaeohydrology. Wiley, Chichester, pp. 527–570.

Beavan, J., Wang, X., Holden, C., Wilson, K., Power, W., Prasetya, G., Bevis, M., Kautoke, R., 2010. Near-simultaneous great earthquakes at Tongan megathrust and outer rise in September 2009. Nature 466, 959–963.

Biester, H., Keppler, F., Putschew, A., Martinez-Cortizas, A., Petri, M., 2004. Halogen retention, organohalogens, and the role of organic matter decomposition on halogen enrichment in two Chilean peat bogs. Environmental Science & Technology 38, 1984–1991.

Blott, S.J., Pye, K., 2006. Particle size distribution analysis of sand-sized particles by laser diffraction: an experimental investigation of instrument sensitivity and the effects of particle shape. Sedimentology 53, 671–685.

Borradaile, G., 1988. Magnetic susceptibility, petrofabrics and strain. Tectonophysics 156, 1–20.

Bridge, J., 2008. Discussion of articles in "Sedimentary features of tsunami deposits". Sedimentary Geology 211, 94.

Cassels, R., 1979. Early prehistoric artefacts from the Waitore site (N136/16) near Patea, Taranaki. New Zealand Journal of Archaeology 1, 85–108.

Chagué-Goff, C., 2010. Chemical signatures of palaeotsunamis: a forgotten proxy? Marine Geology 271, 67–71.

Chagué-Goff, C., Fyfe, W.S., 1996. Geochemical and petrographical characteristics of a domed bog, Nova Scotia: a modern analogue for temperate coal deposits. Organic Geochemistry 24 (2), 141–158.

Chagué-Goff, C., Goff, J., 1999. Geochemical and sedimentological signature of catastrophic saltwater inundations (tsunami), New Zealand. Quaternary Australasia 17, 38–48.

Chagué-Goff, C., Dawson, S., Goff, J., Zachariasen, J., Berryman, K., Garnett, D., Waldron, H., Mildenhall, D., 2002. A tsunami (ca. 6300 years BP) and other Holocene environmental changes, northern Hawke's Bay, New Zealand. Sedimentary Geology 150, 89–102.

Chagué-Goff, C., Goff, J.R., Dominey-Howes, D., Nott, J., Sloss, C., Shaw, W., Law, L., 2011. Tropical Cyclone Yasi and its predecessors. Australian Tsunami Research Centre Miscellaneous Report No. 5, 16 pp. http://www.nhrl.unsw.edu.au.
Cushman, J.A., 1924. Samoan foraminifera. Carnegie Institution of Washington Publication 21, 1–75.
Dahanayake, K., Kulasena, N., 2008. Recognition of diagnostic criteria for recent- and paleo-tsunami sediments from Sri Lanka. Marine Geology 254, 180–186.
Dawson, S., 2007. Diatom biostratigraphy of tsunami deposits: examples from the 1998 Papua New Guinea tsunami. Sedimentary Geology 200, 328–335.
Dawson, A.G., Shi, S., 2000. Tsunami deposits. Pure and Applied Geophysics 157, 875–897.
Dawson, A.G., Stewart, I., 2007. Tsunami deposits in the geological record. Sedimentary Geology 200, 166–183.
Dawson, A.G., Long, D., Smith, D.E., 1988. The Storrega slides: evidence from eastern Scotland for a possible tsunami. Marine Geology 82, 271–276.
Dawson, A.G., Foster, I.D.L., Shi, S., Smith, D.E., Long, D., 1991. The identification of tsunami deposits in coastal sediment sequences. Science of Tsunami Hazards 9 (1), 73–82.
Dawson, A.G., Stewart, I., Morton, R.A., Richmond, B.M., Jaffe, B.E., Gelfenbaum, G., 2008. Reply to Comments by Kelletat (2008) comments to Dawson, A.G. and Stewart, I. (2007) tsunami deposits in the geological record [Sedimentary Geology, 200, 166–183]. Sedimentary Geology 211, 92–93.
Debenay, J.-P., Payri, C.E., 2010. Epiphytic foraminiferal assemblages on macroalgae in reefal environments of New Caledonia. Journal of Foraminiferal Research 40 (1), 36–60.
Dominey-Howes, D., Thaman, R., 2009. UNESCO — IOC International Tsunami Survey Team Samoa (ITST Samoa). Interim Report of Field Survey 14th–21st October 2009. UNESCO—IOC and Australian Tsunami Research Centre Miscellaneous Report No. 2, Sydney.
Dominey-Howes, D., Dawson, A.G., Smith, D.E., 1998. Late Holocene coastal tectonics at Falasarna, western Crete: a sedimentary study. In: Stewart, I.S., Vita-Finzi, C. (Eds.), Coastal Tectonics: Geological Society of London, Special Publication, 146, pp. 343–352.
Dominey-Howes, D., Humphreys, G., Hesse, P., 2006. Tsunami and palaeotsunami depositional signatures and their potential value in understanding the late-Holocene tsunami record. The Holocene 16, 1095–1107.
Ellwood, B.B., Hrouda, F., Wagner, J., 1988. Symposia on magnetic fabrics: introductory comments. Physics of the Earth and Planetary Interiors 51, 249–252.
Etienne, S., Buckley, M., Paris, R., Nandasena, A.K., Clark, K., Strotz, L., Chagué-Goff, C., Goff, J., Richmond, B., 2011. The use of boulders for characterising past tsunamis: lessons from the 2004 Indian Ocean and 2009 South Pacific tsunamis. Earth-Science Reviews 107, 75–89 (this issue).
Fritz, H.M., Kongko, W., Moore, A., McAdoo, B., Goff, J.R., Harbitz, C., Uslu, B., Kalligeris, N., Suteja, D., Kalsum, K., Titov, V., Gusman, A., Latief, H., Santoso, E., Sujoko, S., Djulkarnaen, D., Sunendar, H., Synolakis, C.E., 2007. Extreme runup from the 17 July 2006 Java tsunami. Geophysical Research Letters 34, L12602. doi:10.1029/2007GL029404.
Gelfenbaum, G., Jaffe, B., 2003. Erosion and sedimentation from the 17 July, 1998, Papua New Guinea tsunami. Pure and Applied Geophysics 106, 1969–1999.
Ghose, B.K., 1977. Paleoecology of the cenozoic reefal foraminifers and algae — a brief review. Palaeogeography, Palaeoclimatology, Palaeoecology 22 (3), 231–256.
Goff, J., Chagué-Goff, C., 1999. A late Holocene record of environmental changes from coastal wetlands: Abel Tasman National Park, New Zealand. Quaternary International 56, 39–51.
Goff, J., Chagué-Goff, C., 2009. Cetaceans and tsunamis — whatever remains, however improbable, must be the truth? Natural Hazards and Earth System Sciences 9, 855–857.
Goff, J.R., Rouse, H.L., Jones, S., Hayward, B., Cochran, U., McLea, W., Dickinson, W., Morley, M., 2000. Evidence for an earthquake and tsunami about 3100–3400 yr ago, and other catastrophic saltwater inundations recorded in a coastal lagoon, New Zealand. Marine Geology 170, 231–249.
Goff, J.R., Chagué-Goff, C., Nichol, S.L., 2001. Palaeotsunami deposits: a New Zealand perspective. Sedimentary Geology 143, 1–6.
Goff, J., McFadgen, B., Chagué-Goff, C., 2004a. Sedimentary differences between the 2002 Easter storm and the 15th-century Okoropunga tsunami, southeastern North Island, New Zealand. Marine Geology 204, 235–260.
Goff, J., Wells, A., Chagué-Goff, C., Nichol, S., Devoy, R., 2004b. The elusive AD 1826 tsunami, South Westland, New Zealand. New Zealand Geographer 60, 28–39.
Goff, J.R., Nichol, S.L., Chagué-Goff, C., Horrocks, M., McFadgen, B., Cisternas, M., 2010a. Predecessor to New Zealand's largest historic trans-South Pacific tsunami of 1868 AD. Marine Geology 275, 155–165.
Goff, J., Nichol, S., Kennedy, D., 2010b. Development of a tsunami database for New Zealand. Natural Hazards 54, 193–208.
Goff, J., Pearce, S., Nichol, S.L., Chagué-Goff, C., Horrocks, M., Strotz, L., 2010c. Multi-proxy records of regionally-sourced tsunamis, New Zealand. Geomorphology 118, 369–382.
Goff, J., Lamarche, G., Pelletier, B., Chagué-Goff, C., Strotz, L., 2011. Predecessors to the 2009 South Pacific Tsunami in the Wallis and Futuna Archipelago. Earth-Science Reviews 107, 90–105 (this issue).
Goto, K., Kawana, T., Imamura, F., 2010. Historical and geological evidence of boulders deposited by tsunamis, southern Ryukyu Islands, Japan. Earth-Science Reviews 102, 77–99.
Hallock, P., 1985. Why are larger foraminifera large? Paleobiology 11, 195–208.
Hamilton, N., Rees, A.I., 1970. The use of magnetic fabric in paleocurrent estimation. In: Runcorn, S.K. (Ed.), Paleogeophysics. Academic Press, London, pp. 445–464.
Hawkes, A.D., Bird, M., Cowie, S., Grundy-Warr, C., Horton, B.P., Shau Hwai, A.T., Law, L., Macgregor, C., Nott, J., Ong, J.E., Rigg, J., Robinson, R., Tan-Mullins, M., Sa, T.T., Yasin, Z., Aik, L.W., 2007. Sediments deposited by the 2004 Indian Ocean Tsunami along the Malaysia–Thailand Peninsula. Marine Geology 242, 169–190.
Hayward, B.W., Grenfell, H.R., Reid, C.M., Hayward, K.A., 1999. Recent New Zealand shallow-water benthic foraminifera: taxonomy, ecologic distribution, biogeography and use in paleoenvironmental assessment. Institute of Geological & Nuclear Sciences monograph (New Zealand Geological Survey Paleontological Bulletin) 21 (75), 14–249.
Hemphill-Haley, E., 1996. Diatoms as an aid in identifying late-Holocene tsunami deposits. The Holocene 6, 439–448.
Higman, B., Bourgeois, J., 2008. Deposits of the 1992 Nicaragua tsunami. In: Shiki, T., Tsuji, Y., Yamazaki, T., Minoura, K. (Eds.), Tsunamiites — Features and Implications. Elsevier, pp. 81–103.
Higman, B., Jaffe, B., 2005. A comparison of grading in deposits from five tsunamis: does tsunami wave duration affect grading patterns? Eos Transactions AGU 86 (52) Fall Meeting Supplement, Abstract T11A-0362.
Hori, K., Kuzumoto, R., Hirouchi, D., Umitsu, M., Janjirawuttikul, N., Patanakanog, B., 2007. Horizontal and vertical variation of 2004 Indian tsunami deposit: an example of two transects along the western coast of Thailand. Marine Geology 239, 163–172.
Hottinger, L., Halicz, E., Reiss, Z., 1993. Recent foraminiferida from the Gulf of Aqaba, Red Sea. Opera Slovenian Academy of Sciences and Arts 33 179 pp.
Hughes, J., Mathewes, R., 2003. A modern analogue for plant colonization of palaeotsunami sands in Cascadia, British Columbia, Canada. The Holocene 13, 877–896.
Hussain, S., Mohan, S., Jonathan, M., 2010. Ostracoda as an aid in identifying 2004 tsunami sediments: a report from SE coast of India. Natural Hazards 55, 513–522.
Jaffe, B., Buckley, M., Richmond, B., Strotz, L., Etienne, S., Clark, K., Watt, S., Gelfenbaum, G., Goff, J., 2011. Flow speed estimated by inverse modeling of sandy sediments deposited by the 29 September 2009 tsunami near Satitoa, east Upolu, Samoa. Earth-Science Reviews 107, 22–36 (this issue).
Jagodziński, R., Sternal, B., Szczuciński, W., Lorenc, S., 2009. Heavy minerals in 2004 tsunami deposits on Kho Khao Island, Thailand. Polish Journal of Environmental Studies 18, 103–110.
Jankaew, K., Atwater, B., Sawai, Y., Choowong, M., Charoentitirat, T., Martin, M., Prendergast, A., 2008. Medieval forewarning of the 2004 Indian Ocean tsunami in Thailand. Nature 455, 1228–1231.
Kamatani, A., 1982. Dissolution rates of silica from diatoms decomposing at various temperatures. Marine Biology 68, 91–96.
Kelletat, D., 2008. Comments to Dawson, A.G. Stewart, I. (2007), Tsunami deposits in the geological record [Sedimentary Geology 200, 166–183]. Sedimentary Geology 211, 87–91.
Kokociński, M., Szczuciński, W., Zgrundo, A., Ibragimow, A., 2009. Diatom assemblages in 26 December 2004 tsunami deposits from coastal zone of Thailand as sediment provenance indicators. Polish Journal of Environmental Studies 18, 93–101.
Kortekaas, S., Dawson, A.G., 2007. Distinguishing tsunami and storm deposits: an example from Martinhal, SW Portugal. Sedimentary Geology 200, 208–221.
Krammer, K., Lange-Bertalot, H., 1986. Süsswasserflora von Mitteleuropa. Bacillariophyceae, Teil i: Naviculaceae. Gustav Fischer Verlag, Stuttgart. 876 pp.
Krammer, K., Lange-Bertalot, H., 1988. Süsswasserflora von Mitteleuropa. Bacillariophyceae Teil ii: Bacillariaceae, Epithemiaceae, Surirellaceae. Gustav Fischer Verlag, Stuttgart. 576 pp.
Krammer, K., Lange-Bertalot, H., 1991a. Süsswasserflora von Mitteleuropa. Bacillariophyceae Teil iii: Centrales, Fragilariaceae, Eunotiaceae. Gustav Fischer Verlag, Stuttgart. 596 pp.
Krammer, K., Lange-Bertalot, H., 1991b. Süsswasserflora von Mitteleuropa. Bacillariophyceae Teil iv: Achnanthaceae. Gustav Fischer Verlag, Stuttgart. 437 pp.
Lamarche, G., Pelletier, B., Goff, J., 2010. Impact of the 29 September 2009 South Pacific tsunami on Wallis and Futuna. Marine Geology 271, 297–302.
Lander, J.F., Whiteside, L.S., Lockridge, P.A., 2003. Two decades of global tsunamis, 1982–2002. Science of Tsunami Hazards 21 (1), 3–82.
Lay, T., Ammon, C.J., Kanamori, H., Rivera, L., Koper, K.D., Hutko, A.R., 2010. The 2009 Samoa–Tonga great earthquake triggered doublet. Nature 466, 964–968.
Liu, B., Saito, Y., Yamazaki, T., Abdeldayem, A., Oda, H., Hori, K., Zhao, Q., 2001. Paleocurrent analysis for the Late Pleistocene–Holocene incised-valley fill of the Yangtze delta, China by using anisotropy of magnetic susceptibility data. Marine Geology 176, 175–189.
Loeblich, A.R., Tappan, H., 1987. Foraminiferal Genera and their Classification. Van Nostrand Reinhold, London.
Mamo, B., Strotz, L., Dominey-Howes, D., 2009. Tsunami sediments and their foraminiferal assemblages. Earth-Science Reviews 96, 263–278.
McLeod, M., Slavich, P., Irhas, Y., Moore, N., Rachman, A., Ali, N., Iskandar, T., Hunt, C., Caniago, C., 2010. Soil salinity in Aceh after the December 2004 Indian Ocean tsunami. Agricultural Water Management 97, 605–613.
Minoura, K., Nakaya, S., 1991. Traces of tsunami preserved in inter-tidal lacustrine and marsh deposits: some examples from northeast Japan. The Journal of Geology 99, 265–287.
Minoura, K., Nakaya, S., Uchida, M., 1994. Tsunami deposits in a lacustrine sequence of the Sanriku coast, northeast Japan. Sedimentary Geology 89, 25–31.
Minoura, K., Gusiakov, V.G., Kurbatov, A., Takeuti, S., Svendsen, J.I., Bondevik, S., Oda, T., 1996. Tsunami sedimentation associated with the 1923 Kamchatka earthquake. Sedimentary Geology 106, 145–154.
Minoura, K., Imamura, F., Takahashi, T., Shuto, N., 1997. Sequence of sedimentation processes caused by the 1992 Flores tsunami: evidence from Babi Island. Geology 25 (6), 523–526.
Minoura, K., Imamura, F., Kuran, U., Nakamura, T., Papadopoulos, G.A., Takahashi, T., Yalciner, A.C., 2000. Discovery of Minoan tsunami deposits. Geology 28, 59–62.

Morton, R.A., Gelfenbaum, G., Jaffe, B.E., 2007. Physical criteria for distinguishing sandy tsunami and storm deposits using modern examples. Sedimentary Geology 200, 184–207.
Morton, R.A., Goff, J.R., Nichol, S.L., 2008. Hydrodynamic implications of textural trends in sand deposits of the 2004 tsunami in Sri Lanka. Sedimentary Geology 207, 59–64.
Nanayama, F., Shigenob, K., Satakea, K., Shimokawaa, K., Koitabashic, S., Miyasakac, S., Ishiic, M., 2000. Sedimentary differences between the 1993 Hokkaido-nansei-oki tsunami and the 1959 Miyakojima typhoon at Taisei, southwestern Hokkaido, northern Japan. Sedimentary Geology 135, 255–264.
Narayana, A.C., Tatavarti, R., Shinu, N., Subeer, A., 2007. Tsunami of December 26, 2004 on the southwest coast of India: post-tsunami geomorphic and sediment characteristics. Marine Geology 242, 155–168.
Nichol, S., Goff, J., Devoy, R., Chagué-Goff, C., Hayward, B., James, I., 2007. Lagoon subsidence and tsunami on the West Coast of New Zealand. Sedimentary Geology 200, 248–262.
Nichol, S.L., Chagué-Goff, C., Goff, J.R., Horrocks, M., McFadgen, B.M., Strotz, L.C., 2010. Geomorphology and accommodation space as limiting factors on tsunami deposition: Chatham Island, southwest Pacific Ocean. Sedimentary Geology 229, 41–52.
Okal, E., Fritz, H., Synolakis, C., Borrero, J., Weiss, R., Lynett, P., Titov, V., Foteinis, S., Jaffe, B., Liu, P.L.-F., Chan, I., 2010. Field survey of the Samoa Tsunami of 29 September 2009. Seismological Research Letters 81, 577–591.
Paris, R., Cachão, M., Fournier, J., Voldoire, O., 2010. Nannoliths abundance and distribution in tsunami deposits: example from the December 26, 2004 tsunami in Lhok Nga (northwest Sumatra, Indonesia). Geomorphologie: Relief, Processus, Environnement 1, 109–118.
Park, C.K., Doh, S.J., Suk, D.W., Kim, K.H., 2000. Sedimentary fabric on deep-sea sediments from KODOS area in the eastern Pacific. Marine Geology 171, 115–126.
Parker, J., 2009. Taxonomy of foraminifera from Ningaloo Reef, Western Australia. Memoirs of the Association of Australasian Palaeontologists, 36, pp. 1–810.
Passega, R., 1957. Texture as characteristic of clastic deposition. American Association of Petroleum Geologists Bulletin 41, 1952–1984.
Passega, R., 1964. Grain size representation by CM patterns as a geological tool. Journal of Sedimentary Petrology 34 (4), 830–847.
Peters, R., Jaffe, B., 2010. Identification of tsunami deposits in the geologic record: developing criteria using recent tsunami deposits. US Geological Survey Open-File Report 2010–1239. 38 pp.
Rees, A.I., 1965. The use of anisotropy of magnetic susceptibility in the estimation of sedimentary fabric. Sedimentology 4, 257–271.
Resig, J.M., 2004. Age and preservation of *Amphistegina* (foraminifera) in Hawaiian beach sand: implication for sand turnover rate and resource renewal. Marine Micropaleontology 50 (3–4), 225–236.
Richmond, B.M., Buckley, M., Etienne, S., Chagué-Goff, C., Clark, K., Goff, J., Dominey-Howes, D., Strotz, L., 2011. Deposits, flow characteristics, and landscape change resulting from the September 2009 South Pacific Tsunami in the Samoan Islands. Earth-Science Reviews 107, 37–50 (this issue).
Ruiz, F., Abad, M., Cáceres, L.M., Rodríguez Vidal, J., Carretero, M.I., Pozo, M., González-Regalado, M.L., 2010. Ostracods as tsunami tracers in Holocene sequences. Quaternary Research 73, 130–135.
Santisteban, J.I., Mediavilla, R., Lopez-Pamo, E., Dabrio, C.J., Ruiz Zapata, M.B., Gil Garcia, M.J., Castano, S., Martinez-Alfaro, P.E., 2004. Loss on ignition: a qualitative or quantitative method for organic matter and carbonate mineral content in sediments? Journal of Paleolimnology 32, 287–299.
Sawai, Y., Jankaew, K., Martin, M.E., Prendergast, A., Choowong, M., Charoentitirat, T., 2009. Diatom assemblages in tsunami deposits associated with the 2004 Indian Ocean tsunami at Phra Thong Island, Thailand. Marine Micropaleontology 73, 70–79.
Schlichting, R., Peterson, C., 2006. Mapped overland distance of paleotsunami: high-velocity inundation in back-barrier wetlands of the central Cascadia margin, U.S.A. The Journal of Geology 114, 577–592.
Sen Gupta, B.K., 1999. Systematics of modern foraminifera. In: Sen Gupta, B.K. (Ed.), Modern Foraminifera. Kluwer Academic, London, pp. 7–36.
Seward-Thompson, B.L., Hails, J.R., 1973. An appraisal of the computation of statistical parameters in grain size analysis. Sedimentology 20, 161–169.
Shi, S., Dawson, A.G., Smith, D.E., 1995. Coastal sedimentation associated with the December 12th, 1992 tsunami in Flores, Indonesia. Pure and Applied Geophysics 144, 175–188.
Smith, D.E., Shi, S., Cullingford, R.A., Dawson, A.G., Dawson, S., Firth, C.R., Foster, I.D.L., Fretwell, P.T., Haggart, B.A., Holloway, L.K., Long, D., 2004. The Holocene Storegga Slide tsunami in the United Kingdom. Quaternary Science Reviews 23, 2291–2321.
Srinivasalu, S., Thangadurai, N., Jonathan, M.P., Armstrong-Altrin, J.S., Ayyamperumal, T., Ram-Mohan, V., 2008. Evaluation of trace-metal enrichments from the 26 December 2004 tsunami sediments along the Southeast coast of India. Environmental Geology 53, 1711–1721.
Sugawara, D., Minoura, K., Imamura, F., 2008. Tsunamis and tsunami sedimentology. In: Shiki, T., Tsuji, Y., Yamazaki, T., Minoura, K. (Eds.), Tsunamiites — Features and Implications. Elsevier, Amsterdam, pp. 9–49.
Sujatha, C., Aneeshkumar, N., Renjith, K., 2008. Chemical assessment of sediment along the coastal belt of Nagapattinam, Tamil Nadu, India, after the 2004 tsunami. Current Science 95, 382–385.
Switzer, A., Jones, B., 2008. Large-scale washover sedimentation in a freshwater lagoon from the southeast Australian coast: sea-level change, tsunami or exceptionally large storm? The Holocene 18, 787–803.
Switzer, A., Pucillo, K., Haredy, R., Jones, B., Bryant, E., 2005. Sea level, storm, or tsunami: enigmatic sand sheet deposits in a sheltered coastal embayment from southeastern New South Wales, Australia. Journal of Coastal Research 21, 655–663.
Szczuciński, W., in press. The post-depositional changes of the onshore 2004 tsunami deposits on the Andaman Sea coast of Thailand. Natural Hazards.
Szczuciński, W., Niedzielski, P., Rachlewicz, G., Sobczyński, T., Ziola, A., Kowalski, A., Lorenc, S., Siepak, J., 2005. Contamination of tsunami sediments in a coastal zone inundated by the 26 December 2004 tsunami in Thailand. Environmental Geology 49, 321–331.
Szczuciński, W., Chaimanee, N., Niedzielski, P., Rachlewicz, G., Saisuttichai, D., Tepsuwan, T., Lorenc, S., Siepak, J., 2006. Environmental and geological impacts of the 26 December 2004 tsunami in coastal zone of Thailand — overview of short and long-term effects. Polish Journal of Environmental Studies 15, 793–810.
Szczuciński, W., Niedzielski, P., Kozak, L., Frankowski, M., Zioła, A., Lorenc, S., 2007. Effects of rainy season on mobilization of contaminants from tsunami deposits left in coastal zone of Thailand by the 26 December 2004 tsunami. Environmental Geology 53, 253–264.
Taira, A., 1989. Magnetic fabrics and depositional processes. In: Taira, A., Masuda, F. (Eds.), Sedimentary Facies in the Active Plate Margin. Terra Scientific Publishing Company (TERRAPUB), Tokyo, pp. 43–77.
Tarling, D.H., Hrouda, F., 1993. The Magnetic Anisotropy of Rocks. Chapman & Hall, London. 218 pp.
Uchida, J.-I., Fujiwara, O., Hasegawa, S., Kamataki, T., 2010. Sources and depositional processes of tsunami deposits: analysis using foraminiferal tests and hydrodynamic verification. Island Arc 19, 427–442.
Wassmer, P., Baumert, P., Lavigne, F., Paris, R., Sartohadi, J., 2007. Faciès et transferts sédimentaires associés au tsunami du 26 décembre 2004 sur le littoral au nord-est de Banda Aceh (Sumatra, Indonésie)/Sedimentary facies and transfer associated with the December 26, 2004 tsunami on the north eastern littoral of Banda Aceh (Sumatra, Indonesia). Géomorphologie: Relief, Processus, Environnement 4, 335–346.
Wassmer, P., Schneider, J.-L., Fonfrège, A.-V., Lavigne, F., Paris, R., Gomez, C., 2010. Use of anisotropy of magnetic susceptibility (AMS) in the study of tsunami deposits: application to the 2004 deposits on the eastern coast of Banda Aceh, North Sumatra, Indonesia. Marine Geology 275, 255–272.
Williams, H., Hutchinson, I., 2000. Stratigraphic and microfossil evidence for Late Holocene tsunamis at Swantown marsh, Whidbey Island, Washington. Quaternary Research 54, 218–227.
Witkowski, A., Lange-Bertalot, H., Metzeltin, D., 2001. Diatom flora of marine coasts 1. Iconographia Diatomologica, Volume 7. A.R.G. Gantner Verlag, Ruggell. 925 pp.
Yawsangratt, S., Szczuciński, W., Chaimanee, N., Chatprasert, S., Majewski, W., Lorenc, S., in press. Evidence of probable paleotsunami deposits on Kho Khao Island, Phang Nga Province, Thailand. Natural Hazards. doi:10.1007/s11069-011-9729-4.